

Climate Change Uncertainty Spillover in the Macroeconomy*

Mike Barnett[‡]

William Brock*

Lars Peter Hansen**

April 2, 2021

Abstract

The design and conduct of climate change policy necessarily confronts uncertainty along multiple fronts. We explore the consequences of ambiguity over various sources and configurations of models that impact how economic opportunities could be damaged in the future. We appeal to decision theory under risk, model ambiguity and misspecification concerns to provide an economically motivated approach to uncertainty quantification. We show how this approach reduces the many facets of uncertainty into a low dimensional characterization that depends on the uncertainty aversion of a decision maker or fictitious social planner. In our computations, we take inventory of three alternative channels of uncertainty and provide a novel way to assess them. These include i) *carbon dynamics* that capture how carbon emissions impact atmospheric carbon in future time periods; ii) *temperature dynamics* that depict how atmospheric carbon alters temperature in future time periods; iii) *damage functions* that quantify how temperature changes diminish economic opportunities. We appeal to geoscientific modeling to quantify the first two channels. We show how these uncertainty sources interact for a social planner looking to design a prudent approach to the social pricing of carbon emissions.

*University of Wisconsin and University of Missouri, Columbia

**University of Chicago

‡Arizona State University

*We thank Shirui Chen, Han Xu and Jiaming Wang for the computational support on his research, and Diana Petrova for the help in preparing this manuscript. Financial support for this project was provided by the Alfred P. Sloan Foundation [grant G-2018-11113]. We thank Kevin Murphy for helpful conversations while preparing this manuscript.

1 Introduction

There are many calls for policy implementation to address climate change based on confidence in our knowledge of the adverse impact of economic activity on the climate, and conversely the negative effects of climate change on economic outcomes. Our view is that the knowledge base to support quantitative modeling in the realm of climate change and elsewhere remains incomplete. While there is a substantial body of evidence supporting the adverse human imprint on the environment, uncertainty comes into play when we build quantitative models aimed at capturing the dynamic transmission of human activity on the climate and on how adaptation to climate change will play out over time. It has been common practice to shunt uncertainty to the background when building and using quantitative models in many policy arenas. To truly engage in “evidence-based policy” requires that we are clear both about the quality of the evidence and the sensitivity to the modeling inputs used to interpret the evidence. The importance of quantifying uncertainty has been stressed and implemented in a variety of scientific settings. Our aim is to explore ways to incorporate this uncertainty for the purposes of making quantitative assessments of alternative courses of action. We see this as much more than putting standard errors on econometric estimates, and we turn to developments in dynamic decision theory as a guide to how we confront uncertainty in policy analysis.

In climate economics, Weitzman (2012), Wagner and Weitzman (2015) and others have emphasized uncertainty in the climate system’s dynamics and how this uncertainty could create fat-tailed distributions of potential damages. Relatedly, Pindyck (2013) and Morgan et al. (2017) find existing integrated assessment models in climate economics to be of little value in the actual prudent policy. We are sympathetic to their skepticism, and are not offering simple repairs to the existing integrated assessment models in this area nor quick modifications to EPA postings for the social cost of carbon. Nevertheless, we still find value in the use of models to engage in a form of “quantitative storytelling.” Instead of proceeding with separate analyses for each such model, we find value in model comparisons and seek a framework for “quantitative storytelling” with multiple models. Our aim is to explore ways to incorporate uncertainty explicitly into policy discussions with a more explicit accounting for the limits to our understanding. Not only is there substantial uncertainty about the economic inputs, but also about the geoscientific inputs.

Drawing on insights from decision theory and asset pricing, Barnett et al. (2020) proposed a framework for assessing uncertainty, broadly-conceived, to include ambiguity over alternative models and the potential form of the misspecification of each. In effect, they suggest methods for conducting structured uncertainty analyses. But their examples scratch the surface of the actual quantitative assessment of uncertainty pertinent to the problem of climate change. In this paper, we explore more systematically the consequences of uncertainty coming from both geo-scientific and economic inputs.

Decision theory provides tractable ways to explore a tradeoff between projecting the “best guess” consequences of alternative courses of action versus “worst possible” outcomes among a set of alternative models. Rather than focusing exclusively on these extremal points, we allow our decision maker to take intermediate positions in accordance with parameters that govern aversions to model ambiguity and potential misspecification. We presume a decision maker confronts many dimensions of uncertainty and engages in a sensitivity analysis. We use the social planner’s decision problem to add structure to this sensitivity analysis and reduce a potentially high-dimensional sensitivity analysis to a very low-dimensional characterization of sensitivity parameterized by aversion to model ambiguity and potential misspecification.

This paper takes inventory of the consequence of alternative sources of uncertainty and provides a novel way to assess it. We consider three specific sources:

- *carbon dynamics* mapping carbon emissions into carbon in the atmosphere
- *temperature dynamics* mapping carbon in the atmosphere into temperature changes
- *economic damage functions* that depict the fraction of the productive capacity that is reduced by temperature changes

We necessarily adopt some stark simplifications to make this analysis tractable. Many of the climate models are of both high dimension and nonlinear. Rather than using those models directly, we rely on outcomes of pulse experiments applied to the models. We then take the outcomes of these pulse experiments as inputs into our simplified specification of the climate dynamics inside our economic model. We follow much of the environmental macroeconomic modeling literature in the use of *ad hoc* static damage functions, and explore the consequences of changing the curvature in these damage functions. Even with these simplifications, our uncertainty analysis is sufficiently rich to show how uncertainty about the alternative channels by which emissions induce economic damages interact in important ways. Modeling extensions that confront heterogeneity in exposure to climate change across regions will also open the door to the inclusion of cross-sectional evidence for measuring potential environmental damages.

We use the social cost of carbon (SCC) as a barometer for investigating the consequences of uncertainty for climate policy. In settings with uncertainty, we depict this as an asset price. The social counterpart to a cash flow is the impulse response from a marginal increase in emissions to a marginal impact on damages induced by climate changes in future time periods. This cash flow is discounted stochastically in ways that account for uncertainty. This follows in part revealing discussions in Golosov et al. (2014) and Cai et al. (2017) who explore some of the risk consequences for the social cost of carbon. We extend this by taking a broader perspective on uncertainty. The common discussion in environmental economics about what “rate” should be used to discount future social costs is ill-posed for the model ambiguity that we feature. Rather than a single

rate, we borrow and extend an idea from asset pricing by representing broadly based uncertainty adjustments as a change in probability over future outcomes for the macroeconomy.

This paper extends previous work by “opening the hood” of climate change uncertainty and exploring which components have the biggest impact on valuation. To simplify the policy analysis, we consider a world with a “fictitious social planner.” Thus, we put to the side important questions pertaining to heterogeneity in the exposure to climate change and to the consequent policy objectives by different decision makers. Instead, we simplify the policy implementation to that of a Pigouvian tax that eliminates the wedge between market valuation and social valuation. We use this setup to illustrate how uncertainty can contribute to social valuation while recognizing the need for further model richness is future research. Our planner confronts risk, model ambiguity, and model misspecification formally and deduces a socially efficient emissions trajectory.

2 Uncertain climate dynamics

In this section, we first describe some very tractable characterizations of cross-model variation in the dynamic responses of temperature to emission pulses. To support our analysis, we then build a simplified stochastic specification of the pulse responses.

2.1 Simple approximations to climate dynamics

Recent contributions to the climate science literature have produced low-dimensional approximations, emulators, and pulse experiments that provide tractable alternatives to full-scale Atmospheric-Oceanic General Circulation Models (AOGCMs) used by climate scientists. These results allow for the inclusion of climate models within economic frameworks in ways that can be informative and revealing. We use the pulse experiment results of Joos et al. (2013) and Geoffroy et al. (2013) across various carbon and climate dynamics models to build the set models we will use in our uncertainty analysis.¹

Joos et al. (2013) report the responses of atmospheric carbon concentration to emission pulses of one hundred gigatons of carbon for several alternative Earth System models. The emission pulse experiments follow a standardized model intercomparison analysis so that outcomes are directly comparable. We use the responses for nine such models to capture the variation and uncertainty present in models of carbon cycle dynamics.

We feed these responses for carbon concentration into log-linear approximations of temperature dynamics constructed by Geoffroy et al. (2013). In accordance with the Arrhenius (1896) equation, these dynamics relate the logarithm of carbon in the atmosphere to future temperature. The parameters that Geoffroy et al. (2013) constructed using their simplified representation differ

¹See Seshadri (2017), Eby et al. (2009), Matthews et al. (2009), and MacDougall et al. (2017) for additional examples of work in this area.

depending on the model being approximated. We use the 16 models listed in the appendix. Thus, we take the nine different atmospheric carbon responses as inputs into the 16 temperature dynamics approximations, giving us a total of 144 different temperature responses to emissions.²

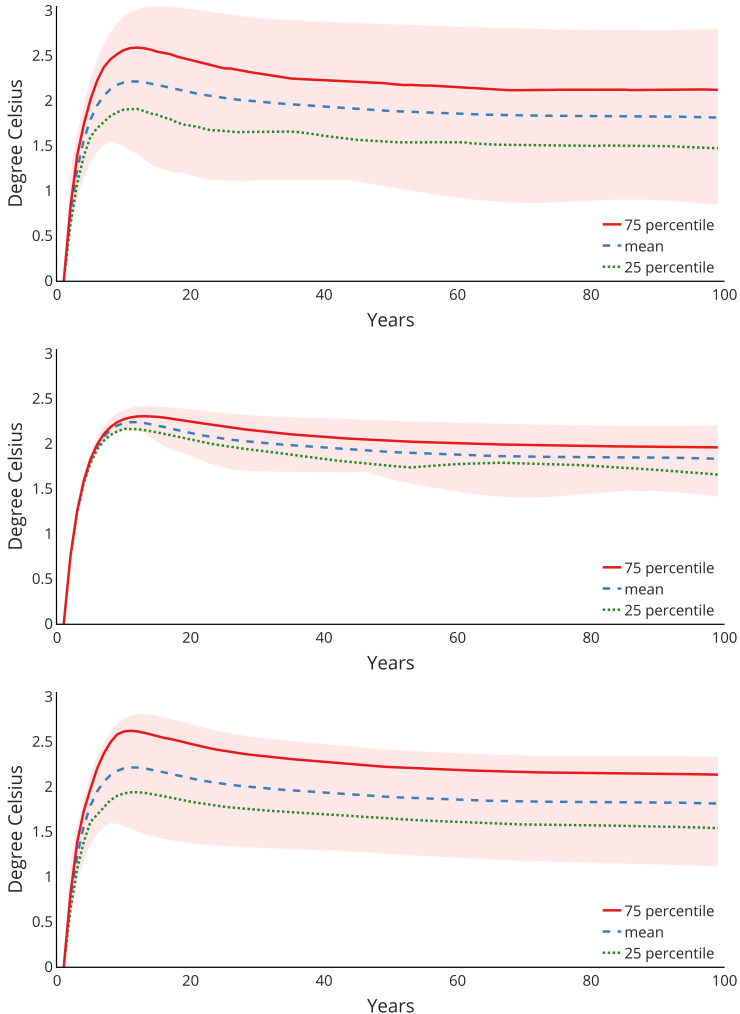


Figure 1: Percentiles for temperature responses to emission impulses. The emission pulse was 100 gigatons of carbon (GtC) spread over the first year. The temperature units for the vertical axis have been multiplied by ten to convert to degrees Celsius per teraton of carbon (TtC). The boundaries of the shaded regions are the upper and lower envelopes. Top panel: percentiles for impulse responses including both carbon and temperature dynamic uncertainty. Center panel: responses obtained for the different carbon responses for nine models each averaged over the 16 models of temperature dynamics. Bottom panel: percentiles for the 16 temperature responses using each averaged over the nine models of carbon concentration dynamics.

²Appendix A provides additional details on the emission pulse responses from Joos et al. (2013), the approximating model of Geoffroy et al. (2013), and lists the specific models we use from these two studies.

Figure 1 captures the resulting temperature responses across various sets of these 144 models. The top panel provides the results based on all 144 models, the middle panel provides the results based on variation in the carbon models, and the bottom panel provides the results based on variation in the temperature models. In each case, the maximal temperature response to an emission pulse occurs at about a decade and the subsequent response is very flat. These dynamics are consistent with the response patterns featured by Ricke and Caldeira (2014).

The top panel of Figure 1 also reports the percentiles for each horizon computed using the 144 different temperature response functions from all the different combinations of models of carbon and temperature dynamics. While there are similar patterns across the temperature response functions, there is considerable heterogeneity in the magnitudes of the responses. For a further characterization of this heterogeneity, we compute the exponentially weighted average of each of these response functions and use them in our computations. We report the resulting histogram as the top panel of Figure 2.

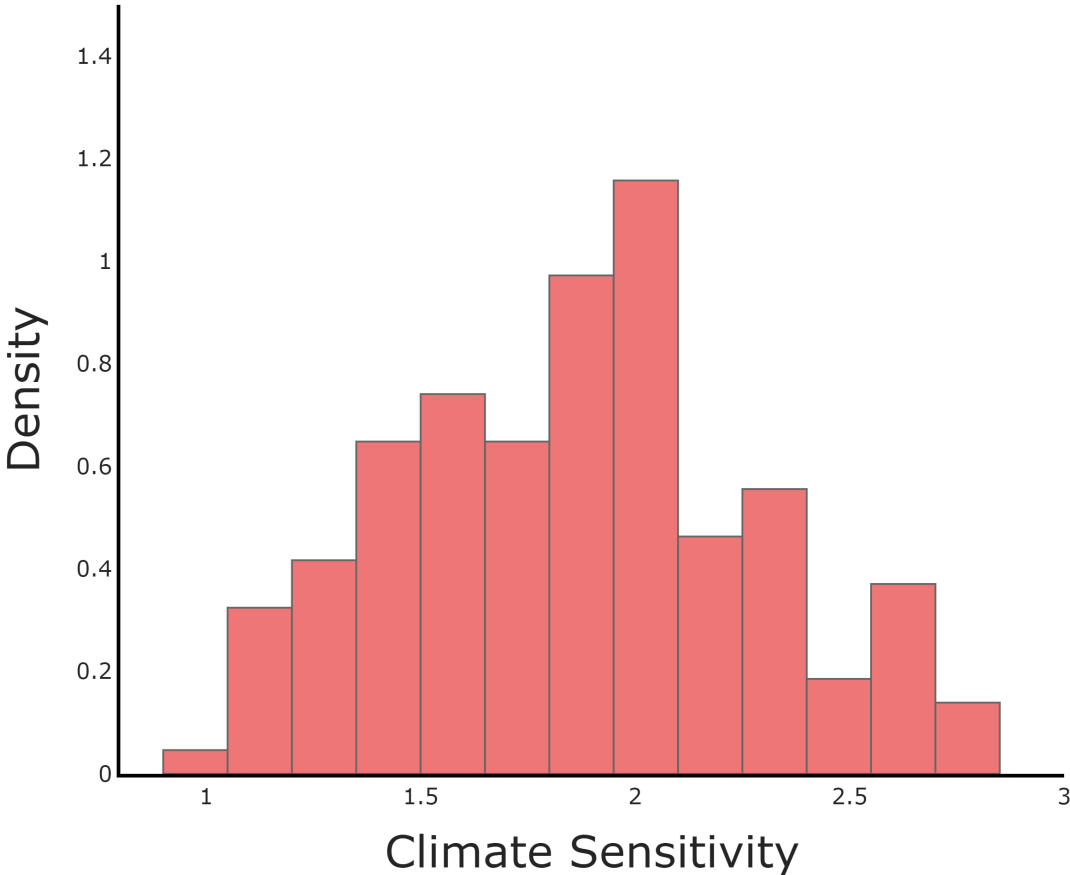


Figure 2: Histograms for the exponentially weighted average responses of temperature to an emissions impulse from 144 different models using a rate $\delta = .01$.

The eventually flat trajectories of the temperature response functions are consistent with model comparisons made using what is called the transient climate response (TCRE) to CO_2 emissions. The TCRE is the ratio of CO_2 -induced warming realized over an interval of time to the cumulative carbon emissions over that same time interval. This linear characterization provides a simplification suggested by Matthews et al. (2009) and others by targeting the composite response of the carbon and temperature dynamics instead of the components that induce it. MacDougall et al. (2017) provide a pedagogical summary of this literature and report a histogram for the TCRE computed for 150 model variants. Their histogram looks very similar to what we report in Figure 2.

The middle and bottom panels of Figure 1 show the contribution of uncertainty in temperature and carbon dynamics to the temperature impulse responses. In generating the middle panel of Figure 1, we computed the implied temperature responses for nine alternative models of atmospheric CO_2 dynamics averaging over the 16 models of temperature dynamics. In generating the lower panel of Figure 1, we computed the 16 temperature responses for 16 temperature models while averaging over the nine models of atmospheric CO_2 dynamics. Consistent with the results reported by Ricke and Caldeira (2014), we find heterogeneity in the temperature responses to be more prominent than that coming from the atmospheric CO_2 dynamics.³

2.2 Stochastic climate pulses

To explore uncertainty, we introduce explicit stochasticity as a precursor to the study of uncertainty. We capture this randomness in part by an exogenous forcing processes that evolves as:

$$dZ_t = \mu_z(Z_t)dt + \sigma_z(Z_t)dW_t$$

where $\{W_t : t \geq 0\}$ a multivariate standard Brownian motion. We partition the vector Brownian motion into two subvectors as follows:

$$dW_t = \begin{bmatrix} dW_t^y \\ dW_t^k \end{bmatrix}$$

where the first component consists of the climate change shocks and the second component contains the technology shocks. Consider an emissions “pulse” of the form

$$(\iota_y \cdot Z_t) \mathcal{E}_t (\theta dt + \varsigma \cdot dW_t^y)$$

where \mathcal{E}_t is fossil fuel emissions and $\iota_y \cdot Z = \{\iota_y \cdot Z_t : t \geq 0\}$ is a positive process which we normalize to have mean one. The $\iota_y \cdot Z$ -process captures “left out” components of the climate

³Ricke and Caldeira (2014) also consider separately two sources of temperature dynamics.

system’s reaction to an emission of \mathcal{E}_t gigatons into the atmosphere while the $\zeta \cdot dW$ process captures short time scale fluctuations. We will use a positive Feller square root process for the $\iota_y \cdot Z$ process in our analysis.

Palmer and Stevens (2019) argue for the systematic inclusion and quantification of stochastic components in climate models as a way to make a substantive improvement in predictive models from climate science, even though the “big picture” is quite settled. Palmer and Stevens proposed modeling improvements that are well beyond the ambition of our work. But we have a shared appreciation for explicit stochastic modeling. It is important for our uncertainty quantification methods that we incorporate explicit randomness to partially disguise the model ambiguity and misspecification from a decision maker.

Within this framework, we impose the “Matthews’ approximation” by making the consequence of the pulse permanent:

$$dY_t = \mu_y(Z_t, \mathcal{E}_t)dt + \sigma_y(Z_t, \mathcal{E}_t)dW_t^y$$

where

$$\begin{aligned}\mu_y(z, e) &= e(\iota_y \cdot z)\theta \\ \sigma_y(z, e) &= e(\iota_y \cdot z)\zeta'\end{aligned}$$

Throughout, we will use uppercase letters to denote random vector or stochastic processes and lower case letters to denote possible realizations. Armed with this “Matthews’ approximation,” we collapse the climate change uncertainty into the cross-model empirical distribution reported in Figure 2. We will eventually introduce uncertainty about θ .

This specification misses the initial build up in the temperature response and instead focuses exclusively on the flat trajectories depicted in the upper panel of Figure 1. We expect that this error might be small when the prudent social planner embraces preferences that have a low rate of discounting the future, but this requires further investigation. While others in climate sciences find linear approximations to be relevant, we recognize the need for subsequent efforts to explore systematically the potential importance of nonlinearities. Ghil and Lucarini (2020) is a thorough review of climate physics at a hierarchy of temporal and spatial scales that embraces the inherent complexity of the climate system.

Remark 2.1. *For a more general starting point, let Y_t be a vector used to represent temperature dynamics where the temperature impact on damages is the first component of Y_t . This state vector evolves according to:*

$$dY_t = \Lambda Y_t dt + \mathcal{E}_t(\iota_y \cdot Z_t)(\Theta dt + \Sigma dW_t^y)$$

where Λ is a square matrix and Θ is a column vector. Given an initial condition Y_0 , the solution

for Y_t satisfies:

$$Y_t = \exp(t\Lambda) Y_0 + \int_0^t \exp[(t-u)\Lambda] (\iota_y \cdot Z_t) \mathcal{E}_t (\Theta dt + \Sigma dW_t^y)$$

Thus under this specification, the expected future response of Y to a pulse at date zero is:

$$\exp(u\Lambda) \Theta.$$

It is the first component of this function that determines the response dynamics. This generalization allows for multiple exponentials to approximate the pulse responses. Our introduction of a multiple exponential approximation adapts for example, Joos et al. (2013) and Pierrehumbert (2014).⁴

As an example, we capture the initial rise in the emission responses by the following two-dimensional specification

$$\begin{aligned} dY_t^1 &= Y_t^2 dt \\ dY_t^2 &= -\lambda Y_t^2 dt + \lambda \theta \mathcal{E}_t dt \end{aligned}$$

which implies the response to a pulse is:

$$\theta [1 - \exp(-\lambda t)] \mathcal{E}_0$$

A high value of λ implies more rapid convergence to the limiting response $\theta \mathcal{E}_0$. This approximation is intended as a simple representation of the dynamics where the second state variable can be thought of as an exponentially weighted average of current and past emissions.⁵

Remark 2.2. The approximation in Geoffroy et al. (2013) includes the logarithm of carbon in the atmosphere as argued for by Arrhenius (1896) which is not directly reflected in the linear approximation to the temperature dynamics that we use. The pulse experiments from Joos et al. (2013) show a more than proportional change in atmospheric carbon when the pulse size is changed. It turns out that this is enough to approximately offset the logarithmic Arrhenius adjustment so that the long-term temperature response remains approximately proportional for small pulse sizes. See

⁴See equation (5) of Joos et al. (2013) and equations (1)-(3) of Pierrehumbert (2014). Pierrehumbert puts the change in radiative forcing equal to a constant times the logarithm of the ratio of atmospheric CO_2 at date t to atmospheric CO_2 at baseline date zero. His Figures 1 and 2 illustrate how an approximation of the Earth System dynamics by three exponentials plus a constant tracks a radiative forcing induced by a pulse into the atmosphere at a baseline date from the atmosphere works quite well with half lives of approximately six, sixty five, and four hundred and fifty years.

⁵In independent work, Dietz and Venmans (2019) and Barnett et al. (2020) have used such simplified approximations within an explicit economic optimization framework. The former contribution includes the initial rapid upswing in the impulse response functions. The latter contribution abstracts from this. Barnett et al. instead explore ways to confront uncertainty, broadly-conceived, while using the Matthews approximation.

also *Pierrehumbert (2014)* who discusses the approximate offsetting impacts of nonlinearity in temperature and climate dynamics.

3 A stochastic model of damages

Our construction of potential damage functions is similar to Barnett et al. with specifications motivated in part by prior contributions. We posit a damage process, N_t , to capture negative externalities on society imposed by carbon emissions. The reciprocal of damages, $\frac{1}{N_t}$, diminishes the productive capacity of the economy because of the impact of climate change.

We use a piecewise log quadratic function for mapping how temperature change induced by emissions alter economic opportunities:

$$\log N_t = \Gamma(Y_t) + \iota_n \cdot Z_t$$

for temperature anomaly Y_t where

$$\Gamma(y) = \gamma_1 y + \frac{\gamma_2}{2} y^2 + \frac{\gamma_3}{2} \mathbf{1}_{y \geq \bar{y}} (y - \bar{y})^2.$$

In this specification, there is a temperature anomaly threshold \bar{y} after which the damage function could become much more curved. This curvature in the “tail” of the damage function is only revealed to decision makers near the threshold. We let the threshold, \bar{y} , equal a temperature anomaly of two degrees centigrade.

To capture damage function uncertainty, we posit a jump process with m absorbing states. Each state corresponds to a value of γ_3 starting at threshold \bar{y} . We denote the possible values as γ_3^m for $m = 1, 2, \dots, M$. We focus on cases where the jump occurs when $Y < \tilde{y} \leq \bar{y}$. At the time of the jump, the right tail of the damage function is revealed via γ_3 whereas prior to the jump this parameter is unknown where each value γ_3^m has prior probability π_m^p . We localize the jump around the threshold \bar{y} , and for some the computations take limits of this where the jump is very likely to occur just prior to hitting the threshold. What is uncertain is the value of γ_3 governing the steepness of the damage until after the jump takes place.

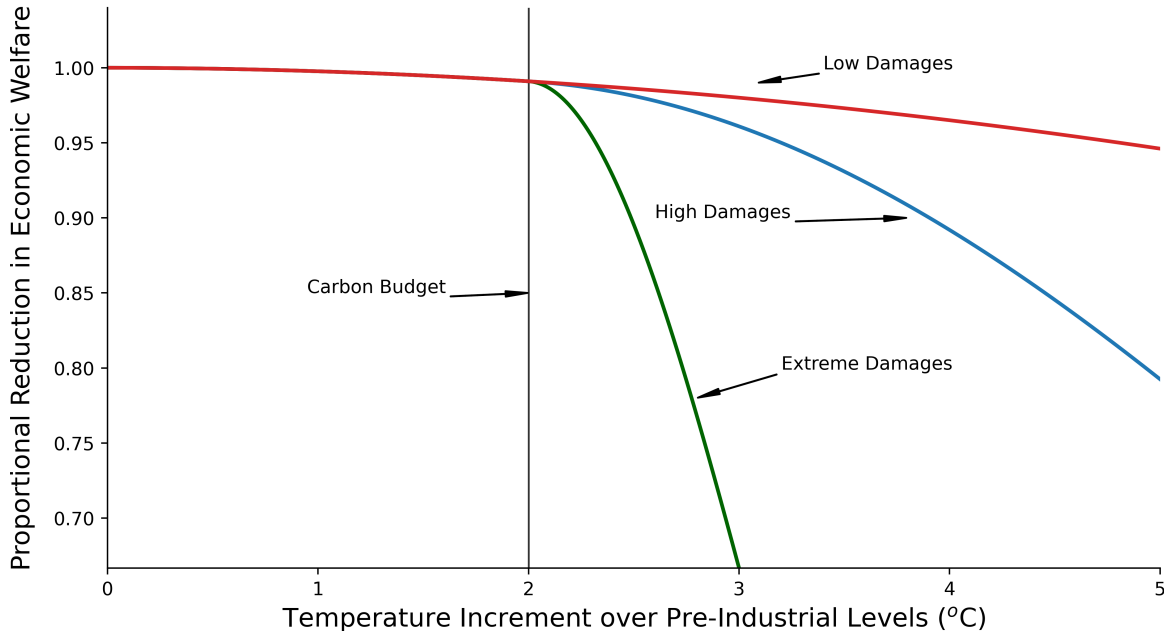


Figure 3: Three possible damage functions. This figure plots $\exp(-n)$, which measures the proportional reduction of the productive capacity of the economy.

In our earlier work, Barnett et al., we consider two specifications of damages motivated by prior research. One specification sets $\gamma_3 = 0$ and sets γ_2 to approximate Nordhaus (2018).⁶ We refer to this as the low damage specification. A second specification sets $\gamma_3 > 0$ to capture the steeper degradation in damages that Weitzman (2012) has argued for. We refer to this as the high damage specification. While Weitzman used uncertainty based on the potential fat tails in the posterior distribution for unknown damage coefficients, we follow Barnett et al. and introduce a high damage possibility and explore how a prudent decision maker should respond to the resulting damage function. We plot the high and low damage functions in Figure 3. Finally, there has been considerable discussion from the geo-sciences of the need to impose a two degree carbon budget. This corresponds to the vertical line in Figure 3. Rather than naively embracing this view, we introduce a third damage function that is much steeper than the high damage function reported in Figure 3 for which there is a one third reduction in the productive capacity of the economy due to a three degree temperature increase. We refer to this as an extreme damage specification. While the term “extreme” may appear to be loaded, we only mean for it to be descriptive as we are not providing new evidence that bears on the probability of any of the three specifications. We use these damage function specifications as an illustration, but our approach is not tied to

⁶Nordhaus (2018) also considered uncertainty around this curve but in a manner that makes our other specifications very unlikely. Later, we will discuss how we will describe how our approach to uncertainty differs from his and other approaches.

these particular damage functions or to baseline probabilities that we assign to them.

Remark 3.1. *The information dynamics here are in contrast to much of the previous research, including Nordhaus (2018), Hassler et al. (2018) and our previous research Barnett et al. (2020), where the analysis is either static or the damage function in the right tail is never revealed.⁷ This jump specification takes a rather different perspective that the curvature is revealed once we cross a threshold. More generally, a rigorous learning-based analysis would be a valuable extension, but it would require that we provide a formal characterization of the precise acquisition of information pertinent to damage function curvature.*

We impose a jump intensity function that is, by design, localized at $y = \bar{y}$:

$$\mathcal{I}(y) = \begin{cases} \left(\frac{1}{\sqrt{2\rho}}\right) \exp\left[-\frac{(y-\bar{y})^2}{2\rho^2}\right] & y < \bar{y} \\ \left(\frac{1}{\sqrt{2\rho}}\right) & y \geq \bar{y} \end{cases}$$

which becomes concentrated in the neighborhood of \bar{y} for ρ small.⁸ A large intensity informs us that a jump is likely. We let π_m^p be the probabilities conditioned on the jump. When the process jumps to state m , the parameter γ_3^m is revealed and the continuation value function is ϕ_m . For sufficiently small ρ , we will approximate the solution to the control problem by deriving an ambiguity adjusted continuation value function at \bar{y} .

4 An illustrative economy

To illustrate our approach to uncertainty, we deliberately use a highly stylized economic model. Later, we will consider two alternative richer specifications of the economic environment necessary to address some important policy challenges.

We start by specifying the economy in the absence of environmental damages. We pose an AK technology for which output is proportional to capital and can be allocated between investment and consumption. Capital in this specification should be broadly conceived. Suppose that there are adjustment costs to capital that are represented as the product of capital times a quadratic function of the investment-capital ratio. Given the output constraint and capital evolution imposed by the AK technology, it suffices to let the planner choose the investment-capital ratio.

⁷Nordhaus (2018) explored the consequences of *date dependent* information revelation in contrast to our *state dependent* revelation.

⁸This intensity is recognizable as the scaled version of half normal density with mean \bar{y} and standard deviation ρ .

Formally, “undamaged” capital evolves as

$$dK_t = K_t \left[\mu_k(Z_t)dt + \left(\frac{I_t}{K_t} \right) dt - \frac{\kappa}{2} \left(\frac{I_t}{K_t} \right)^2 dt + \sigma_k(Z_t)dW_t^k \right]$$

where K_t is the capital stock and I_t is investment. The capital evolution expressed in logarithms is

$$d \log K_t = \left[\mu_k(Z_t) + \left(\frac{I_t}{K_t} \right) - \frac{\kappa}{2} \left(\frac{I_t}{K_t} \right)^2 \right] dt - \frac{|\sigma_k(Z_t)|^2}{2} dt + \sigma_k(Z_t)dW_t^k,$$

where K_t is the capital stock. Consumption and investment are constrained to be:

$$C_t + I_t = \alpha K_t$$

where C_t is consumption.

Next, we consider environmental damages. We suppose that temperature shifts proportionately consumption and capital by a multiplicative factor N_t that captures damages to the productive capacity induced by climate change. For instance, the damage adjusted consumption is $\tilde{C}_t = \frac{C_t}{N_t}$ and the damage adjusted capital is $\tilde{K}_t = \frac{K_t}{N_t}$. Notice that:

$$d \log \tilde{K}_t = d \log K_t - d \log N_t$$

Thus, damages induce a deterioration of the capital stock.

Consumer/investor preferences are time-separable with a unitary elasticity of substitution with an instantaneous time t contribution:

$$\begin{aligned} & (1 - \eta) \log \tilde{C}_t + \eta \log \mathcal{E}_t \\ & = (1 - \eta)(\log C_t - \log N_t) + \eta(\log K_t - \log N_t) + \eta \log \mathcal{E}_t \end{aligned}$$

We let δ be the subjective rate of discount used in preferences.

Remark 4.1. *The model as posed has a solution that conveniently separates. We may solve two separate control problems i) determines “undamaged” consumption, investment and capital ii) determines emissions, the temperature anomaly and damages. It is the latter one that is of particular interest. Undamaged consumption, investment and capital are merely convenient constructs that allow us to simplify the model solution.*

5 Uncertainty aversion

The model we have built so far is one in which uncertainty is captured by the stochastic specification of shocks as is typical when building dynamic stochastic models in macroeconomics. We

think of this shock specification as characterizing *risk*. The presence of these shocks opens the door to a comprehensive assessment of uncertainty in which we entertain a broader notion of uncertainty. We include uncertainty over model specifications and parameters, which we refer to as ambiguity. In this discussion, we treat models and parameters as synonymous by thinking of each parameter as indexing an alternative model. We are led to depart from the Bayesian approach which starts with the specification of a subjective prior over the alternative models, but does not distinguish the role of subjective probabilities over models from the probabilities given a model. Instead, we use recent formalisms from decision theory under uncertainty to explore the impact of uncertainty over the subjective inputs. Within statistics, this gave rise to robust counterparts to Bayesian inferences in the study of prior sensitivity, often outside the realm of a specific decision problem. The decision theory framework formalizes the question of “sensitivity to what?” and the formal tradeoff between making best guesses versus possible bad outcomes as we look across models. While in some settings, data richness may diminish the role of prior sensitivity, we find the economics of climate change to be a problem whereby prior sensitivity remains an important question for the decision maker. Of course, any model we write down is necessarily a simplification. We also incorporate concerns about the potential *misspecification* of the models under exploration using ideas from robust control theory extended to dynamic economic models.

Our use of decision theory gives rise to a form of uncertainty quantification. Uncertainty quantification in the sciences is typically done by researchers. For instance, we might ask how the social cost of carbon differs as we change the modeling ingredients. But decision makers also confront this uncertainty, including ones inside the models that we build. Thus, model ambiguity or misspecification concerns by decisions makers should arguably be taken into account when determining the prudent course of action. This same uncertainty emerges as adjustments to the social cost of carbon as set by say a benevolent social planner. Just like risk aversion can induce caution in decision making, the same can be said of broader notions of uncertainty aversion. While the decision theory that we use does not determine the magnitude of what this aversion should be, it reduces a potentially high dimensional sensitivity analysis to a much lower dimensional one captured by low dimensional representations of uncertainty aversion.

We analyze this uncertainty using the formalism of decision theory under uncertainty. We apply two versions of such theory, one comes under the heading of variational preferences and the other under smooth ambiguity preferences. We adapt both to continuous-time specifications, which facilitates their implementation and interpretation. We use this decision theory to reduce the sensitivity analysis to a one or two-dimensional parameterization that locates the potential misspecification that is most consequential to a decision maker. Our aim is to provide a more complete uncertainty quantification within the setting of decision problems.

5.1 Other approaches to uncertainty quantification across models

We briefly discuss three prior forms of uncertainty quantification as it pertains to unknown parameters or models. We give these as illustrations, but the list is by no means exhaustive.

Olson et al. (2012) propose and implement a Bayesian method for making inferences about certain parameters of interest, including a climate sensitivity parameter coming from the UVic (University of Victoria) earth system climate model. They document posterior sensitivity of the climate sensitivity parameter to priors and other unknown modeling inputs. In particular, they show the need to use an informative prior for climate sensitivity to obtain reasonable results, therefore demonstrating the posterior uncertainty in their informative statistical investigation. While not the focal point of their analysis, there is additional uncertainty in the likelihood construction. These forms of uncertainty are pertinent not only to researchers presenting evidence, but also to decision or policy makers as they make decisions. Thus, we move the uncertainty quantification “inside the decision problem,” including the sensitivity analysis. This allows us to explore the impact of model or parameter ambiguity for choosing socially prudent emissions trajectories and imputing the implied social cost of carbon.

In an alternative investigation of uncertainty in a climate economic model, Nordhaus (2018) computes distributions of model outcomes given *a priori* distributions of parameters, specifications and model inputs, including emissions pathways. From their analysis, they are able to produce a set of outputs associated with each parameter or model configuration to demonstrate the role of uncertainty in their setting. Their static analysis occurs “outside the decision problem,” but it opens the door to exploring changes in the prior probability distribution without a systematic analysis of the sensitivity. Our framework uses recursive methods and decision theoretic tools to determine endogenously prudent choices of emissions over time and the implied social cost of carbon trajectories when the policy maker confronts prior ambiguity. Policy outcomes include endogenous feedbacks and dynamic impacts on the social cost of carbon, and, importantly, an adjustment for uncertainty that is either unresolved, or only resolved well into the future.⁹

In a third approach, Hassler et al. (2018) conduct an analysis of uncertainty by comparing policy outcomes across two parameter intervals, one pertaining to damages and another to climate sensitivity. Instead of putting a probability distribution over parameters, they evaluate policy outcomes at the extreme points of parameter space. Their analysis can be thought of as a simple illustration of robust decision making allowing for arbitrary probabilities over the unknown parameters and is a revealing starting point to the policy problem they investigate. Our analysis of the policy problems is explicitly dynamic and imposes probabilistic restraints on the probabilities that could be assigned over a potentially large set of alternative model configurations. The

⁹Nordhaus (2018) noted the inability of his framework to address such endogenous feedbacks and unresolved uncertainty, and highlights the potential value to using the type of recursive methods we employ in our analysis as a way to address such issues.

dynamic decision theory formulation we use collapses our resulting sensitivity analysis to a low dimensional representation in terms of ambiguity and misspecification aversion parameters.

5.2 Components of uncertainty

Posing our model in continuous-time leads to a simplified characterization of robustness. Given our interest in recursive methods, in what follows, we will describe in turn implications for misspecifying a Brownian motion, a jump process and an ambiguity adjustment for the local mean of the dynamical system. We will then explore a more structured approach that allows us to target uncertainty in how to weight alternative models of climate dynamics. Since this also leads us to assess implications for the local mean, we may make direct comparisons between a more structured approach to model ambiguity and a less structured approach exploring potential model misspecification.¹⁰

5.2.1 Misspecified Brownian motion

Following James (1992), Hansen and Sargent (2001) and others, the potential misspecification of a Brownian motion has a particularly simple form. It is known from the famed Girsanov Theorem that a change in distribution represented by a likelihood ratio for Brownian motions induces a drift distortion. Under such a change in probability distribution, dW_t is changed from a Brownian increment to a Brownian increment with a drift or local mean that can be state (or model) dependent, which we denote $H_t dt$. Thus, to explore the consequences of misspecification, we modify our (locally) normally distributed shocks by entertaining possible mean distortions. Entertaining arbitrary changes in the drift without a constraint or a penalty, leads to an uninteresting and inflexible decision problem. Here we follow one of the preference specifications in Hansen and Sargent, which is also a continuous-time version of dynamic variational preferences of Maccheroni et al. (2006), whereby we use an expected log-likelihood ratio measure of discrepancy called relative entropy to restrain the search over alternative possible drift specifications. For Brownian motion models, the relative entropy penalty is $\frac{\xi_b}{2}|H_t|^2 dt$ where ξ_b is penalty parameter that governs the decision maker concern for misspecification and $\frac{1}{2}|H_t|^2 dt$ is the local contribution to relative entropy. This formulation leads to a straightforward adjustment to a Hamilton-Jacobi-Bellman equation used for continuous-time optimization.

Let ψ denote a value function defined as a function of a Markov state X_t . Suppose the local Brownian contribution to the state evolution dX_t is $\sigma_x(X_t)dW_t$. Then a drift distortion $H_t dt$ contributes $\left(\frac{\partial\psi(X_t)}{\partial x}\right) \cdot (\sigma_x H_t) dt$ to the value function evolution. As part of recursive robustness

¹⁰See Hansen and Sargent (2020b) and Cerreia-Vioglio et al. (2021) for decision theoretic discussions of the distinct roles for model ambiguity and misspecification concerns.

adjustment, we solve

$$\min_h \left(\frac{\partial \psi}{\partial x} \right) \cdot (\sigma_x h) + \frac{\xi_b}{2} |h|^2.$$

The solution to this minimization problem is:

$$h^* = -\frac{1}{\xi_b} \sigma_x' \left(\frac{\partial \psi}{\partial x} \right) \quad (1)$$

with minimized objective:

$$-\frac{1}{2\xi_b} \left(\frac{\partial \psi}{\partial x} \right)' \sigma_x \sigma_x' \left(\frac{\partial \psi}{\partial x} \right). \quad (2)$$

The solution h^* locates the direction, $\sigma_x' \left(\frac{\partial \psi}{\partial x} \right)$ that alters the local evolution of the value function in the most adverse manner, and it scales this direction inversely with the penalty parameter ξ_b . The implied change in the local evolution for $d\psi(X_t)$ is

$$-\frac{1}{\xi_b} \left(\frac{\partial \psi}{\partial x} \right)' \sigma_x \sigma_x' \left(\frac{\partial \psi}{\partial x} \right)$$

We impose an aversion to the misspecification of Brownian risk by including the term (2) in the HJB equation.

5.2.2 Misspecified jump process

To specify a Markov jump process requires both a) a state-dependent intensity governing the probability of a jump and b) the distribution over the post jump state. Both of these could be mistaken. We capture both forms of potential misspecification by introducing positive random variables $G_t^m \geq 0$ for each alternative damage model m with local evolution of the state given by

$$\mathcal{I}(Y_t) \sum_{m=1}^M G_t^m \pi_m^p [\psi_m - \psi]$$

where π_m^p , for $m = 1, 2, \dots, M$ are the baseline probabilities and $\mathcal{I}(Y_t)$ is the baseline intensity for the jump process. The altered probabilities resulting from the concern about misspecification are given by

$$\frac{G_t^m \pi_m^p}{\bar{G}_t} \quad m = 1, 2, \dots, M$$

where \bar{G}_t is a normalization defined by

$$\bar{G}_t \doteq \sum_{m=1}^M G_t^m \pi_m^p;$$

and the altered intensity of the jump process is given by $\mathcal{I}(Y_t)\bar{G}_t$.

Thus the choice of the G_t^m 's alters both the jump probabilities and the jump intensities in a manner that is mathematically tractable. The local relative entropy discrepancy for a jump process is:

$$\mathcal{I}(Y_t) \sum_{m=1}^M \pi_m^p (1 - G_t^m + G_t^m \log G_t^m) \geq 0$$

This measure is nonnegative because the convex function $g \log g$ exceeds its gradient $g-1$ evaluated at $g = 1$.

To determine a local contribution to an HJB equation, we follow Anderson et al. (2003) by solving

$$\min_{g^m \geq 0: m=1,2,\dots,M} \mathcal{I} \sum_{m=1}^M g^m \pi_m^p (\psi_m - \psi) + \xi_p \mathcal{I} \sum_{m=1}^M \pi_m^p (1 - g^m + g^m \log g^m)$$

where $\xi_p > 0$ is a penalty parameter limiting the search over the G_t^m 's with realized values given by the g^m 's. The minimizers are:

$$g_m^* = \exp \left[\frac{1}{\xi_p} (\psi - \psi_m) \right],$$

which do not depend directly on the intensity \mathcal{I} .¹¹ Notice that the g_m^* tilt exponentially towards the states for which the post jump value function ψ_m is low relative to the pre jump value function ψ . The implied minimized objective is:

$$\xi_p \mathcal{I} \sum_{m=1}^M \pi_m^p \left(1 - \exp \left[\frac{1}{\xi_p} (\psi - \psi_m) \right] \right) = -\xi_p \mathcal{I} \frac{\sum_{m=1}^M \pi_m^p \exp \left(-\frac{1}{\xi_p} \psi_m \right) - \exp \left(-\frac{1}{\xi_p} \psi \right)}{\exp \left(-\frac{1}{\xi_p} \psi \right)}$$

We add this outcome to the HJB equation of the decision maker to adjust for robustness to jumps misspecification.

5.2.3 Local ambiguity aversion

To assess the consequences of the heterogeneous responses from alternative climate models, we use what are called recursive smooth ambiguity preferences proposed by Klibanoff et al. (2009). For an important special case of these preferences, Hansen and Sargent (2007) provide a robust prior/posterior interpretation of these preferences. This alternative interpretation has advantages both in terms of calibration and representation of social valuation. In deploying such preferences, we use a robust prior interpretation in conjunction with the continuous-time formulation of smooth ambiguity proposed by Hansen and Miao (2018).

¹¹The value function ψ does depend implicitly on the intensity, which in turn alters the distorted intensity.

In our application, we will entertain L alternative climate models, and will confront ambiguity in what weights to assign to these L models. To be specific, suppose that we have L different climate models where the local mean or drift is μ_x^ℓ for model ℓ . Let π_ℓ^a denote the baseline probability of drift model L . Standard model averaging would use:

$$\sum_{\ell=1}^L \pi_\ell^a \mu_x^\ell$$

as the drift for decision making. Our decision maker is uncertain, however, about what weights to assign but uses an initial set of weights as a baseline. For instance, in our computations we will treat a collection of models with equal probability under a baseline and look for a robust adjustment to these probabilities. Under the robust prior/posterior interpretation of the smooth ambiguity model, the decision maker with value function ψ solves:

$$\min_{\pi_\ell, \ell=1,2,\dots,L} \sum_{\ell=1}^L \pi_\ell \left[\left(\frac{\partial \psi}{\partial x} \right) \cdot \mu_x^\ell + \xi_a (\log \pi_\ell - \log \pi_\ell^a) \right] \quad (3)$$

where ξ_a is a penalty parameter used to restrain the search over the weights to assign to the alternative models. The minimizing probabilities satisfy:

$$\omega_\ell^a \propto \pi_\ell^a \exp \left[-\frac{1}{\xi_a} \left(\frac{\partial \psi}{\partial x} \right) \cdot \mu_x^\ell \right],$$

where the minimizing probabilities are reweighted based on the implied value function drift for model ℓ . Small values of the penalty parameter ξ_a result in an enhanced re-weighting. The minimized objective is:

$$-\xi_a \log \sum_{\ell=1}^L \pi_\ell^a \exp \left[-\frac{1}{\xi_a} \left(\frac{\partial \psi}{\partial x} \right) \cdot \mu_x^\ell \right]$$

In contrast to the robustness adjustment used for model misspecification, this approach adds more structure to the drift distortions to the evolution $d\psi(X_t)$:

$$\begin{aligned} \left(\frac{\partial \psi}{\partial x} \right) \cdot \left[\sum_{\ell=1}^L (\omega_\ell^a - \pi_\ell^a) \mu_x^\ell \right] & \quad \text{smooth ambiguity} \\ -\frac{1}{\xi_b} \left(\frac{\partial \psi}{\partial x} \right)' \sigma_x \sigma_x' \left(\frac{\partial \psi}{\partial x} \right) & \quad \text{misspecification} \end{aligned}$$

We have introduced three different parameters (ξ_b, ξ_p, ξ_a) that guide our sensitivity analysis. From a decision theoretic perspective, these are “preference parameters” that govern aversion to uncertainty broadly conceived. Anderson et al. (2003) impose that $\xi_b = \xi_p$ and suggest ways to calibrate the robustness component based on statistical detection challenges. Since our application of smooth ambiguity and misspecified Brownian motion induce drift distortions for the value

function, we can set the penalty parameters (ξ_b, ξ_p) so that the drift distortions for the continuation values are comparable. Finally, for the calibration of the smooth ambiguity parameter, we are guided by an approach from robust Bayesian analysis attributed to Good (1952) that inspects the implied distortions for *a priori* plausibility.

In our pedagogical discussion so far, we have seemingly ignored possible interactions between damage uncertainty and climate uncertainty. In fact, these interactions will be present as climate change uncertainty will impact the value function contributions given by the ψ_m 's and by ψ . Moreover, the continuation value functions, ψ_m , that condition on damage function curvature contribute to the boundary condition for ψ pertinent when the temperature anomaly is less than the threshold.

5.3 A valuation adjustment for uncertainty

There is much discussion in the literature on environmental economics about what discount rate to use. In our analysis so far, there is a single discount rate used to define the preferences of a fictitious social planner. But the discussions in the literature usually refer to present discounted value formulas for marginal valuation. We represented the robust adjustments in terms of altered probabilities which we compute in conjunction with the HJB equations used for optimization. As Barnett et al. (2020) demonstrate, these same probabilities provide the uncertainty adjustments for social valuation. Thus, to account for uncertainty, broadly conceived, we are pushed beyond the question of what discount rate to use because the necessary adjustment is most conveniently depicted as an altered probability measure.

6 A climate component of a planner's decision problem

To illustrate how uncertainty can impact the analysis of a climate economic system, we consider the partial differential equations that provide a recursive characterization of the value function. As we indicated previously, these partial differential equations take the form of HJB equations. As we explain in Appendix B, the planners value function is additively separable with components that can be computed separately. We focus here on the component that includes the emissions as a control and the temperature anomaly and damages as states. Let $\tilde{\mathcal{E}}_t = (\iota_y \cdot Z_t) \mathcal{E}_t$, which we will use as a transformed control variable.

We start with the equation for value function contribution, $\psi(y, n) = \phi(y) + \frac{(\eta-1)}{\delta} n$. The HJB

equation of interest for $y < \bar{y}$ prior to Poisson jump is:

$$\begin{aligned}
0 = \max_{\tilde{e}} & -\delta\phi(y) + \eta \log \tilde{e} \\
& + \frac{d\phi(y)}{dy} \sum_{\ell=1}^L \pi_{\ell}^{\alpha} \theta_{\ell} \tilde{e} + \frac{1}{2} \frac{d^2\phi(y)}{(dy)^2} |\varsigma|^2 \tilde{e}^2 \\
& + \frac{(\eta-1)}{\delta} \left[(\gamma_1 + \gamma_2 y) \sum_{\ell=1}^L \pi_{\ell}^{\alpha} \theta_{\ell} \tilde{e} + \frac{1}{2} \gamma_2 |\varsigma|^2 \tilde{e}^2 \right] \\
& + \mathcal{I}(y) \sum_{m=1}^M \pi_m^p [\phi_m(y) - \phi(y)]
\end{aligned} \tag{4}$$

The second and third lines include the terms for the dynamics for y and n respectively. The fourth line gives the jump contribution.

The first-order conditions for emissions are:

$$\frac{\eta}{\tilde{e}} = -\frac{d\phi(y)}{dy} \sum_{\ell=1}^L \pi_{\ell}^{\alpha} \theta_{\ell} - \frac{d^2\phi(y)}{(dy)^2} |\varsigma|^2 \tilde{e} - \frac{(\eta-1)}{\delta} \left[(\gamma_1 + \gamma_2 y) \sum_{\ell=1}^L \pi_{\ell}^{\alpha} \theta_{\ell} + \gamma_2 |\varsigma|^2 \tilde{e} \right]. \tag{5}$$

Recall that $\tilde{e} = (\iota_y \cdot z)e$. Multiplying (5) by $\iota_y \cdot z$,

$$\begin{aligned}
\frac{\eta}{e} = & -\frac{d\phi(y)}{dy} (\iota_y \cdot z) \sum_{\ell=1}^L \pi_{\ell}^{\alpha} \theta_{\ell} - (\iota_y \cdot z)^2 \frac{d^2\phi(y)}{(dy)^2} |\varsigma|^2 e \\
& - \frac{(\eta-1)}{\delta} \left[(\iota_y \cdot z) (\gamma_1 + \gamma_2 y) \sum_{\ell=1}^L \pi_{\ell}^{\alpha} \theta_{\ell} + (\iota_y \cdot z)^2 \gamma_2 |\varsigma|^2 e \right]
\end{aligned} \tag{6}$$

In terms of cost-benefit accounting, we think of the left side of (6) as the marginal benefit and the right side as the marginal cost induced because emissions today alter temperature and damages in the future. These latter impacts are conveniently represented in terms of marginal contributions of current period emissions on the value function evolution expressed as function of (y, n) . In what follows, when we evaluate the emissions along the socially optimal trajectory, we exploit the equating of marginal benefits to marginal costs and use the right side of (6) to represent the social cost of carbon. When we impose a decision rule for emissions that is not optimal, we will continue to use the right side of (6) to represent the social cost of carbon.¹² There is a counterpart to this

¹²Given our recursive formulation, we are naturally led to think in terms of policy rules. If there is an allocation rule for emissions as a function of the state of the climate, albeit one that is inefficient, then this feedback will alter ϕ and hence its derivative with respect to temperature. This feedback could come from market/policy interactions not spelled out here. With this feedback and outside of a setting where we can apply the Envelope Theorem, the right side necessarily takes account of how future changes in the climate impact future emissions and not just damages. Moreover, feedback in emissions alters the climate dynamics. Given these considerations, the right side of equation (6) is perhaps better conceived as a measure of future net costs based on future considerations. This allocative feedback is in contrast to an exogenously specified path of emissions independent of the future climate

formula that holds when the planner confronts model ambiguity and misspecification concerns.

Equation (4) is expressed in terms of the pre jump contribution ϕ to the value function. It depends on the continuation value functions ϕ_m pertinent after the tail of damage function is realized. These continuation value functions solve equations:

$$0 = \max_{\tilde{e}} -\delta\phi_m(y) + \eta \log \tilde{e} \\ + \frac{d\phi_m(y)}{dy} \sum_{\ell=1}^L \pi_\ell^a \theta_\ell \tilde{e} + \frac{1}{2} \frac{d^2\phi_m(y)}{(dy)^2} |\varsigma|^2 \tilde{e}^2 \\ + \frac{(\eta-1)}{\delta} \left([\gamma_1 + \gamma_2 y + \gamma_3^m (y - \bar{y})] \sum_{\ell=1}^L \pi_\ell^a \theta_\ell \tilde{e} + \frac{1}{2} (\gamma_2 + \gamma_3^m) |\varsigma|^2 \tilde{e}^2 \right)$$

for $m = 1, 2, \dots, M$.

Given the localized nature of the jump intensity, we expect

$$\phi(\bar{y}) \approx \sum_{m=1}^M \pi_m^p \phi_m(\bar{y}).$$

where the approximation becomes more accurate as ρ becomes small. For our computations without uncertainty adjustments, we consider the limiting case in which this approximation is imposed as a boundary condition when $y = \bar{y}$.

To explore the consequences of uncertainty and sensitivity to some of the subjective inputs, we add the following terms to the equations of interest:

- Brownian misspecification: include

$$-\frac{1}{2\xi_b} \left| \left[\frac{d\phi(y)}{dy} + \frac{(\eta-1)}{\delta} (\gamma_1 + \gamma_2 y) \right] \right|^2 |\varsigma|^2 \tilde{e}^2.$$

- Jump misspecification: replace $\mathcal{I}(y) \sum_{m=1}^M \pi_m^p [\phi_m(y) - \phi(y)]$ with:

$$-\xi_p \mathcal{I} \frac{\sum_{m=1}^M \pi_m^p \exp\left(-\frac{1}{\xi_p} \phi_m\right) - \exp\left(-\frac{1}{\xi_p} \phi\right)}{\exp\left(-\frac{1}{\xi_p} \phi\right)}$$

- Climate model ambiguity: replace

$$\sum_{\ell=1}^L \pi_\ell^a \theta_\ell \left[\frac{d\phi(y)}{dy} + \frac{(\eta-1)}{\delta} (\gamma_1 + \gamma_2 y) \right] \tilde{e}$$

anomalies. The commonly posed exogenous trajectories would lead to a different computation of the social cost of carbon.

with ambiguity adjusted certainty equivalent:

$$-\xi_a \log \sum_{\ell=1}^L \pi_\ell^a \exp \left(-\frac{1}{\xi_a} \theta_\ell \left[\frac{d\phi(y)}{dy} + \frac{(\eta-1)}{\delta} (\gamma_1 + \gamma_2 y) \right] \tilde{e} \right)$$

In what follows, we will impose these terms separately and together with the first and second or second and third. The first and third give unstructured and structured ways to impose drift distortions. While their comparison is interesting, we see little rationale to impose both of them simultaneously. When the uncertain jump adjustment is made, we expect:

$$\phi(\bar{y}) \approx -\xi_p \log \sum_{m=1}^M \pi_m^p \exp \left[-\frac{1}{\xi_p} \phi_m(\bar{y}) \right]$$

where the right side is the certainty equivalent for an ambiguity adjusted post jump continuation value. For our computations with uncertainty adjustments, we impose this as a boundary value. A list of parameters we hold fixed for the computations that follow are given in Appendix B. Figure 4 illustrates the “value matching” that we imposed where the blue dashed line is the certainty equivalent continuation value function with a robust adjustment for model misspecification. In this figure, the certainty equivalent used in the value matching is lower than even the high damage model but still distant from the extreme value model. In the next section, we will have more to say about the parameter settings for ξ_b, ξ_p, ξ_a .

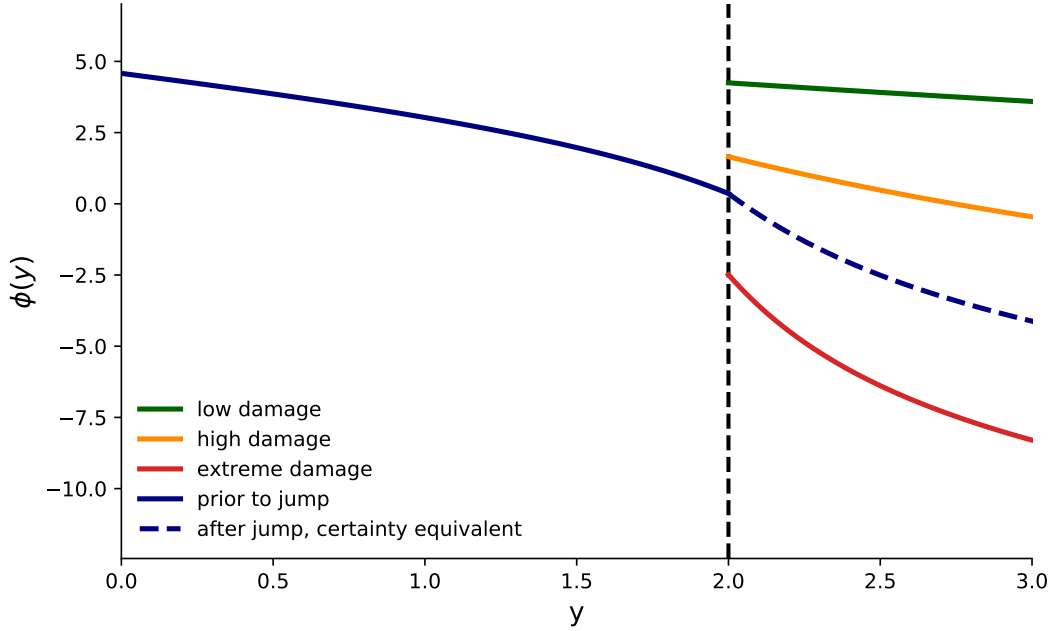


Figure 4: Continuation value function for a model with jump misspecification and ambiguity aversion. Baseline probabilities for damage functions are $1/3, 1/3, 1/3$.

The logarithm of the social cost of carbon has three components:

$$\log SCC_t = \log C_t - \log N_t - \log \mathcal{E}_t + [\log \eta - \log(1 - \eta)] \quad (7)$$

where $\log C_t$ is the fictitious undamaged consumption and grows approximately linearly with quantiles that have different approximate slopes. This component will remain the same across our calculations. We will feature the second and third contributions as they vary with the aversions to uncertainty.

7 Sensitivity

While the penalty parameters (ξ_b, ξ_p, ξ_a) provide a convenient way to represent the consequence of uncertainty aversion, their numerical values are hard to interpret directly. For this reason, we will follow in part the lead of the robust Bayesians by finding it revealing to inspect the plausibility of the implied minimizing probabilities. These altered probabilities are not intended to be the beliefs of a social planner, but rather they reflect how large the misspecification concern is in the assignment of the benchmark probabilities. If such probabilities are easily dismissed as being too extreme, then the penalty parameters were set too low. Anderson et al. (2003) complement this

approach by asking how challenging it would be for a statistician to distinguish the worst-case model from the baseline model with data histories of different lengths.

7.1 Robust perspective

We initially abstract from smooth ambiguity by essentially setting $\xi_a = \infty$. In the continuous time robustness framework of Anderson et al. (2003), the penalty parameters ξ_b and ξ_p are equal, which leaves us with one parameter. As they also note, there is a preference equivalence between a concern for model misspecification and risk aversion in the recursive utility formulation of Kreps and Porteus (1978) and Epstein and Zin (1989) when there is a unitary elasticity of substitution as we have assumed here. Our macroeconomic model, by design, can capture what is called “long-run risk” in the macro-finance literature in the absence of climate change. See Bansal and Yaron (2004). The long-run risk literature explores the valuation consequence of growth rate uncertainty using a recursive utility model of investor preferences. The preference specification presumes a full commitment to the baseline probabilities, but the rationale for this commitment appears to be weak when confronting specific forms of growth rate uncertainty. The long-run risk literature often imposes a seemingly large risk aversion parameter that arguably can look more plausible when reinterpreted as a concern of model misspecification.

We start by imposing $\xi_p = \xi_b = 5$. The implied risk aversion under recursive utility is twenty one, which is certainly large but typically not dismissed as too large in the empirical literature on long-run risk. The Brownian drift induced by a robustness concern is negligible, but there is a notable re-weighting of the three damage functions. We plot the altered probabilities over damage models in Figure 5. Not surprisingly, the probabilities are ordered depending upon the severity of the damage specification. The probability on the extreme damage specification is monotone increasing in the temperature anomaly. While Brownian drift adjustment for misspecification is very small for the temperature, it is quite sizable for the counterpart adjustment to the consumption/capital dynamics. Borrowing and updating a specification of growth rate uncertainty of Hansen et al. (2008), Hansen and Sargent (2020a) fit a simple consumption/capital model to aggregate data designed to measure macroeconomic growth-rate uncertainty. Their model is the undamaged version of the model we pose here, with two shocks. One shock is to the stochastic process for growth rate productivity and the other is an independent shock to only the capital productivity. These shocks imply two of the consumption shocks in Bansal and Yaron (2004).¹³

¹³Bansal and Yaron (2004) also include a shock to stochastic volatility that we abstract from here and consider implications for changing the intertemporal elasticity of substitution.

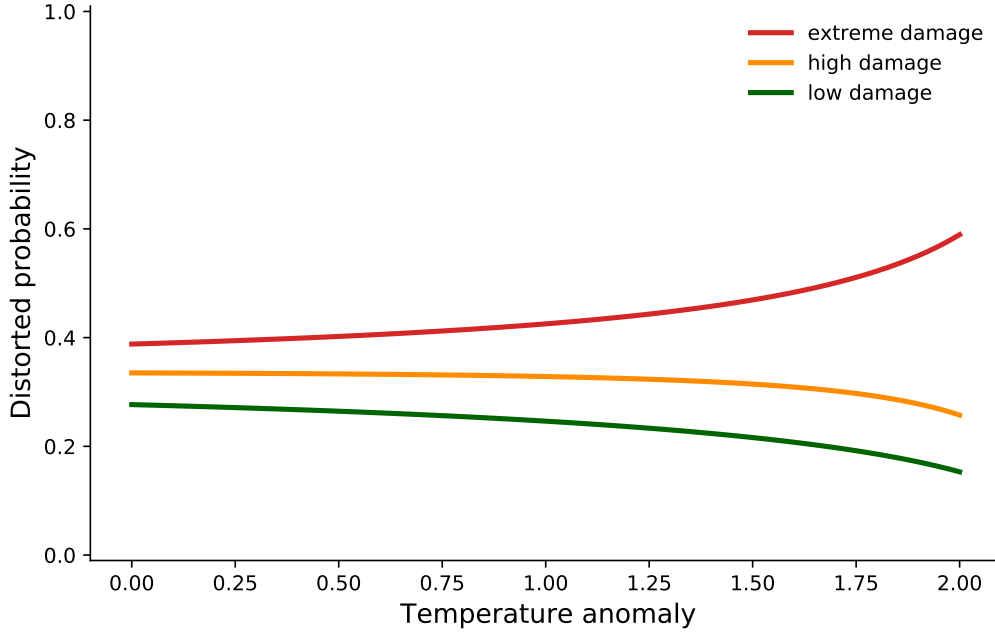


Figure 5: Distorted probabilities of damage functions for a model with Brownian motion and jump misspecification. $\xi_b = \xi_p = 5$. Baseline probabilities for damage functions are $1/3, 1/3, 1/3$.

The implied drift distortions for the stochastic capital evolution are:

$$h = \begin{bmatrix} -.715 \\ -.170 \end{bmatrix} \quad \begin{array}{l} \text{productivity growth rate shock distortion} \\ \text{capital productivity shock distortion.} \end{array}$$

While temperature distortions are negligible, the long-run risk model leaves the door open to much more sizable distortions, particularly for macroeconomic growth-rate uncertainty. Given the relative magnitudes of the adjustments, it is the growth uncertainty channel that is of particular importance to the decision maker. Though .715 is large in comparison to the unit standard deviation of the shock, should we double the penalty parameter ξ_b this number would be about half the size, and we would still get a notable slanting of the damage function specification probabilities. While we find this comparison between misspecification and risk aversion in the presence of growth rate uncertainty to be revealing, an uncomfortable feature of the long-run risk formulation in the macro asset pricing literature is that the long-run risks are a bit of a “black box.”

Remark 7.1. *to assess the magnitude of the distortion, Anderson et al. (2003) suggest to mea-*

asuring the implied magnitude of the statistical divergence measure of Chernoff (1952). Chernoff computed the asymptotic decay rate in mistakenly distinguishing one model from another given a history of data. When the decay rate is small, the models are hard to tell apart from data. It is an ex ante measure of distance between probability models. Since the implied Brownian motion drift distortions show very little state dependence and diffusions are locally normal, the Chernoff rate is approximately

$$\text{Chernoff} = \frac{|h|^2}{8} = .068$$

The half life associated with this is about ten years. Doubling the penalty parameter ξ_b would increase this half life to be about forty.

Statistical divergence measures seem less relevant when applied to our Poisson jump limit and its penalization parameter ξ_p . Given that we effectively restricted the process to a single jump, there is a very limited role for learning about the potential misspecification.

We now put aside the growth uncertainty channel in the long-run risk model and focus on the uncertainty in the temperature dynamics and damage function specification. Moreover, the statistical challenges for the geo-scientific inputs look quite different than those pertinent to determining the alternative damage specifications. For this reason, we break the link between ξ_p and ξ_b by allowing for a much smaller penalty ξ_b while leaving $\xi_p = 5$. We report results for $\xi_b = 0.3$ with the implied drift distortion of .114. This distortion is essentially constant as a function of the state variable and hence over time. A smaller value of ξ_b will induce a larger change in the drift.¹⁴

We consider another configuration in which $\xi_b = \xi_p = 0.3$. With a ξ_p parameter of this magnitude, the tilted probabilities load up almost entirely on the extreme damage specification while the Brownian distortion remains essentially at .114.

We report the emissions trajectories for four configurations of robustness penalties in Figure 6:

- baseline: $\xi_b = \xi_p = \infty$;
- $\xi_b = \xi_p = 5$;
- $\xi_b = 0.3, \xi_p = 5$;
- $\xi_b = 0.3, \xi_p = 0.3$.

The lower three trajectories show how a misspecification averse planner chooses to emit more slowly.

¹⁴The half life of the Chernoff entropy for this distortion is about 400 years.

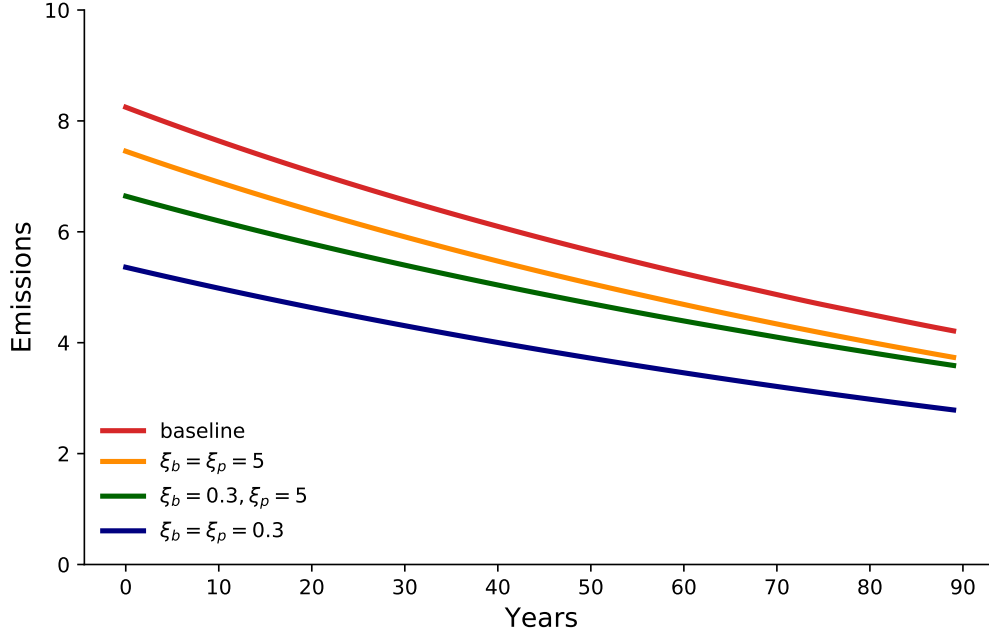


Figure 6: Emissions trajectories under different penalty configurations. The trajectories are simulated under the baseline probabilities abstracting from the intrinsic randomness.

Figure 7 reports the logarithm of the implied social cost of carbon net of stochastic growth contribution contributed by “undamaged consumption.” Specifically, this figure plots trajectories for

$$\log C_0 - \log N_t - \log \tilde{\mathcal{E}}_t + \log \eta - \log(1 - \eta)$$

under the evolution implied by the baseline probabilities. In comparing this formula to formula (7), the one used for the figure abstracts from the stochastic contributions induced by Brownian motion and by fluctuations in $\iota_y \cdot Z_t$ and is translated at date zero so that its exponential at the initial date is comparable with other measures of the social cost of carbon. From this figure, we see that the additional uncertainty increases this cost by about twenty percent as measured by the difference in logarithms times one hundred. The omitted consumption component is common to all of the calculations and its inclusion would not alter the logarithmic differences.

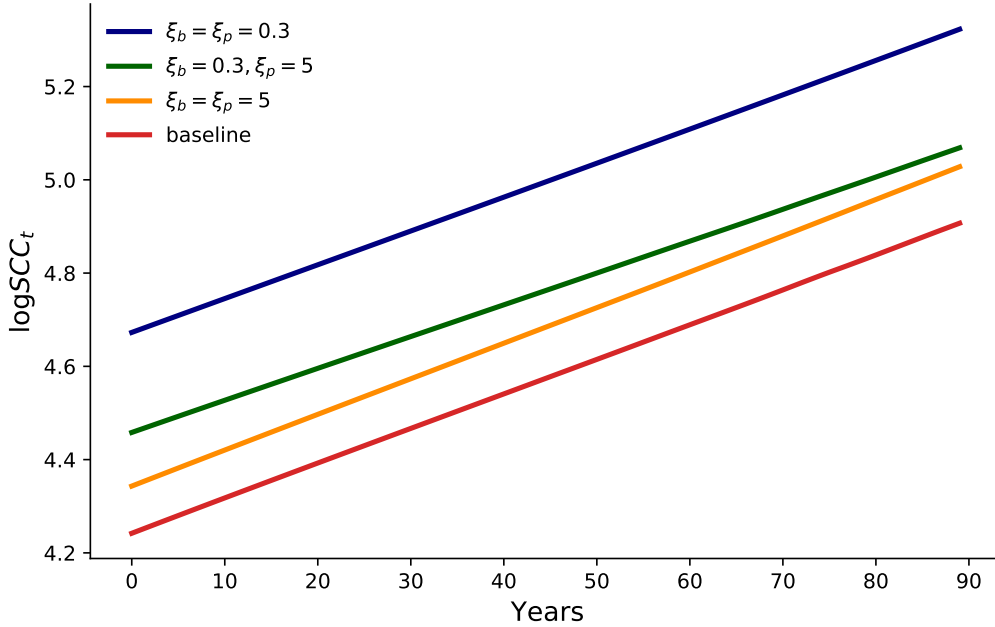


Figure 7: Social cost of carbon expressed in logarithms. The trajectories are computed with baseline probabilities and simulated with zero Brownian risk.

7.2 Structured climate uncertainty

A possible source of the drift distortion is the uncertainty over the climate sensitivity parameter implied by the alternative models. This leads us now to replace the unstructured drift distortion with changes in how we weight the alternative climate models by closing down the drift distortion channel by effectively setting $\xi_b = \infty$ and activating the smooth ambiguity channel. For this example, the Brownian distortion can be interpreted as a mean shift in the temperature dynamics. Specifically, the drift distortion that we computed when $\xi_b = 0.3$ would be equivalent to a mean shift of about .25 in the histogram reported in Figure 2. This opens the door more structured interpretation of the misspecification concern and opens the door to uncertainty decomposition that we explore in the next section.

In the computations that follow, we set $\xi_a = .01$. This numerical value itself has little meaning. What is of more interest is the implied adjustment in the probabilities for the θ_ℓ parameters associated with the 144 climate models. Recall that our baseline probabilities assign equal weight to all 144 models. Figure 8 shows both the original histogram (in red) and the altered histogram (in blue). As we expect, there is a shift to the right towards larger values of θ_ℓ , but arguably not in an extreme fashion. While we allow for the altered histograms to depend on the state y , in

fact we find very little variation in our calculations. The implied mean shift in the distribution is essentially the same as that implied by the unstructured drift distortion. In effect, the tilted histogram provides an interpretation for the robust drift distortion since we essentially chose the penalty parameter $\xi_a = .01$ to achieve this outcome.¹⁵ We chose the penalty parameter $\xi_a = .01$ in part to achieve this outcome. The implied emissions and social cost of carbon trajectories will be essentially the same as those depicted in Figures 6 and 7.

Decreasing ξ_a will lead to a larger shift upwards in the distribution of cross model climate values of θ_ℓ 's.

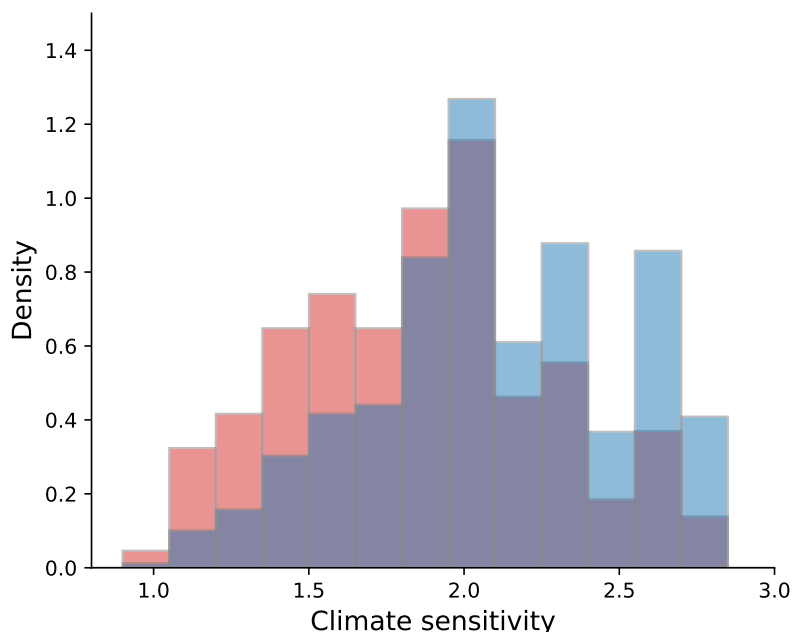


Figure 8: Histograms of climate sensitivity parameters. The red histogram is the outcome of equally weighting all 144 climate models. The blue histogram is the outcome of the minimization in our social planners problem.

Remark 7.2. *We explored two extensions that turned out to have little quantitative consequence. First, we introduced a second state variable as proposed in Remark 2.1. The additional state variable was included to accommodate the initial rise in the impulse response of temperature to an emissions pulse. Including this state variable with a half life of 6 years had very minor consequences for emissions or the social cost of carbon. The second extension we explored was adding a Hotelling (1931) constraint on the stock of reserves. Except for the low damage specification,*

¹⁵For an example in which the structured uncertainty does simply imitate a model misspecification concern see Hansen and Sargent (2020a).

a Hotelling constraint has a negligible impact on our computations. *McGlade and Ekins (2015)* provided estimates of fossil fuel resources or potential reserves, i.e., fossil fuels that are or will be recoverable at any time with current or future technology. Using a value of reserves of 3000 GtC, nearly the same as the baseline quantity from the *McGlade and Ekins* analysis, and at the very low end of potential reserves estimates they provide, we find almost no Hotelling constraint impact on our results. This insensitivity is consistent with results from our endogenous reserve model in *Barnett et al. (2020)*. Were we instead to impose a carbon budget constraint divorced from the stock of reserves, this could have a substantial impact, but we view this as an even more extreme damage function.

8 Uncertainty decomposition

An advantage to the more structured approach implemented as smooth ambiguity is that it allows us to “open the hood” so-to-speak on uncertainty. We build on the work of *Ricke and Caldeira (2014)* by exploring the relative contributions of uncertainty in the carbon dynamics versus uncertainty in the temperature dynamics. We depart from their analysis by studying the relative contributions in the context of a decision problem. We include the damage specification as a third source of uncertainty. We use the social cost of carbon as a benchmark for assessing these contributions. For the uncertainty decomposition, we hold fixed the emissions trajectory and hence also the implied damage trajectory and explore the consequences of imposing constraints on minimization over the probabilities across the different models.

Let P_j for $j = 1, 2, \dots, J$ be a partition of the positive integers up to L . We will choose these partitions to correspond to alternative models of carbon dynamics and temperature dynamics. We previously discussed how to implement ambiguity aversion by solving minimization problem (3). We now extend this idea to partitions of the uncertainty components. For any given such partition, we solve a constrained version of the minimization problem (3) by targeting the probabilities assigned to partitions while imposing the benchmark probabilities conditioned on each partition:

$$\begin{aligned} \min_{\bar{\pi}_j, j=1, 2, \dots, J} & \left(\frac{\partial \psi}{\partial x} \right) \cdot \sum_{j=1}^J \bar{\pi}_j \sum_{\ell \in P_j} \left(\frac{\pi_\ell^a}{\sum_{\ell \in P_j} \pi_\ell^a} \right) \mu_x^\ell \\ & + \xi_a \sum_{j=1}^J \bar{\pi}_j (\log \bar{\pi}_j - \log \bar{\pi}_j^a) \end{aligned}$$

where:

$$\frac{\pi_\ell^a}{\sum_{\ell \in P_j} \pi_\ell^a} \quad \ell \in P_j$$

are the baseline conditional probabilities for partition j . We only minimize the probabilities across

partitions while imposing the baseline conditional probabilities within a partition. The two states in our problem are $x = (y, n)$ and we look for a value function of the form $\psi(y, n) = \phi(y) + \frac{(\eta-1)}{\delta}n$ while imposing that $\tilde{\epsilon} = \epsilon(y)$. For each partition of interest, we construct the corresponding HJB equation that supports this minimization. As before, we impose a boundary condition at the threshold $y = \bar{y}$, and we activate robustness adjustments for the damage function specification in the same way as we have done previously.

From the first-order conditions for $\tilde{\epsilon}$ under the baseline probabilities, we can represent:

$$\frac{\eta}{\tilde{\epsilon}} = -\frac{d\phi(y)}{dy} \sum_{\ell=1}^L \pi_{\ell}^a \theta_{\ell} - \frac{d^2\phi(y)}{(dy)^2} |\varsigma|^2 \tilde{\epsilon} + \frac{(1-\eta)}{\delta} \left[(\gamma_1 + \gamma_2 y) \sum_{\ell=1}^L \pi_{\ell}^a \theta_{\ell} + \gamma_2 |\varsigma|^2 \tilde{\epsilon} \right]. \quad (8)$$

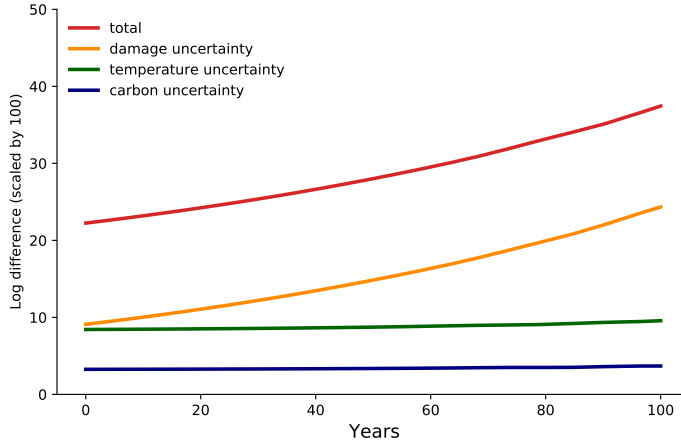
The formula on the right-hand side implicitly encodes expectations of the future captured by the value function derivatives. Indeed, the social cost of carbon can be viewed as a forward-looking asset price with an adverse social cash flow. Conveniently, when we activate ambiguity and robustness adjustments, an analogous formula holds but with the worst-case probabilities replacing the baseline probabilities. In effect, we are using the worst-case (subject to penalization) probabilities in the valuation. For instance, under the structured uncertainty specification:

$$\frac{\eta}{\tilde{\epsilon}} + \frac{d\phi(y)}{dy} \sum_{\ell=1}^L \omega_{\ell}^a \theta_{\ell} + \frac{d^2\phi(y)}{(dy)^2} |\varsigma|^2 \tilde{\epsilon} + \frac{(\eta-1)}{\delta} \left[(\gamma_1 + \gamma_2 y) \sum_{\ell=1}^L \omega_{\ell}^a \theta_{\ell} + \gamma_2 |\varsigma|^2 \tilde{\epsilon} \right] = 0.$$

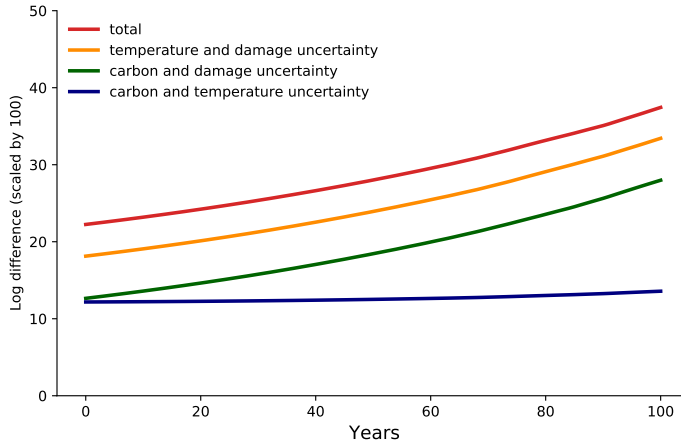
where the ω_{ℓ}^a 's are minimizing probabilities.

When we impose $\tilde{\epsilon} = \epsilon(y)$ and solve constrained minimization problems with respect to probabilities, the equality will cease to hold at minimized probabilities. Nevertheless, the right side of (8) continues to reflect the change in probabilities both directly and indirectly through the computation of ϕ . For our uncertainty decomposition, we compute the logarithm of this expression for alternative partitions of the models. We start by activating separately uncertainty aversion over the i) models of carbon dynamics, ii) the models of temperature dynamics and iii) the models or economic damages. In each case we report the difference in logarithms between the computation using the baseline probabilities and the solutions from the constrained probability minimizations. Importantly, we change both probabilities and value functions in this computation. The results are reported in Figure 9a. For comparison we include the analogous computation when we activate an aversion to all three sources of uncertainty. From this figure, we see that the uncertainty adjustments in valuation account for twenty to thirty percent of the social cost of carbon. With the penalties, $\xi_p = 5$ and $\xi_a = .01$, the contributions from temperature are essentially constant over time with the temperature uncertainty contribution being substantially larger. The damage contribution is initially well below half the total uncertainty, but this changes to more than half after one hundred years. It is important to remember that these computations are performed

while imposing the planner’s solution for emissions and damages. So called “business-as-usual” simulations would change substantially this uncertainty accounting.



(a) The uncertainty partitions account separately for temperature, carbon and damage specifications.



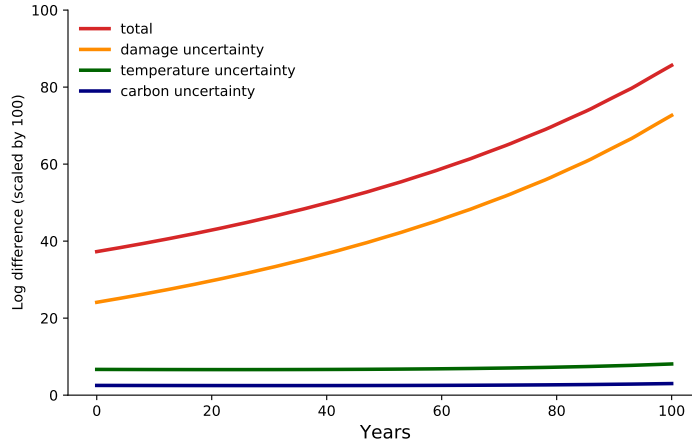
(b) The uncertainty partitions account for combinations of temperature, carbon and damage specifications.

Figure 9: Uncertainty decomposition for the logarithm of the marginal value of emissions (scaled by 100). These computations impose $\xi_a = .01$ and $\xi_p = 5$. The figures report log differences between marginal values computed with baseline probabilities and corresponding values constructed with probabilities minimized over the corresponding partitions.

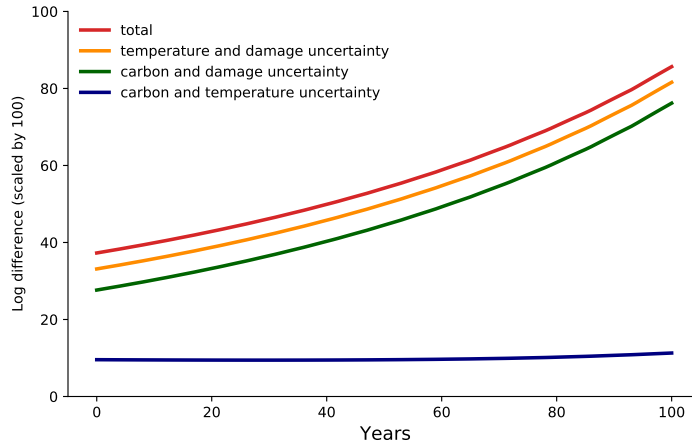
Since the uncertainty components are not “additive,” we explore the joint impacts by partitioning the uncertainty using the three different pairings of contributions. The results are reported in Figure 9b. Not surprisingly, the combination of temperature and damage uncertainty has the

biggest impact accounting for about three-fourths of the total uncertainty. In contrast, the combination of temperature and carbon uncertainty accounts for somewhere between one-half and one-third of the total uncertainty depending on how many years in the future we look at.

The quantitative importance of damages will increase as we reduce ξ_p . We see the ξ_p setting as dictating how much wiggle room a decision maker wants to entertain for the weighting of the alternative damage model specifications. For comparison, we set $\xi_p = 0.3$ to match what we used previously for ξ_b . With this change, minimizing probabilities are shifted almost entirely to the “extreme damage” specification, given us effectly an upper bound on the uncertainty contribution to the social cost of carbon. Now the overall uncertainty contribution ranges from thirty to sixty percent as shown in Figure 10a. The damage uncertainty contribution alone accounts for more than half of this where as the temperature and climate contributions remain about the same as before. Temperature and damage uncertainty taken together account for most of the uncertainty as reflected in Figure 10b.



(a) The uncertainty partitions account separately for temperature, carbon and damage specifications.



(b) The uncertainty partitions account for combinations of temperature, carbon and damage specifications.

Figure 10: Uncertainty decomposition for the logarithm of the marginal value of emissions (scaled by 100). These computations impose $\xi_a = .01$ and $\xi_p = .3$. The figures report log differences between marginal values computed with baseline probabilities and corresponding values constructed with probabilities minimized over the corresponding partitions.

Remark 8.1. *The uncertainty decomposition we implement depends on the underlying emissions trajectory we impose. For the reported computations, we used the planner’s solution for when all uncertainty components are considered. Since our planner cares about uncertainty, robustness considerations lead our planner to avoid excessive exposure to uncertainty when possible. In our particular setting, with uncertainty aversion the planner will prefer to avoid being vulnerable to*

damage function uncertainty, which can be achieved in part by delaying when the potentially steep slope of the damage function becomes operative. Yet, the exposure components of uncertainty can look very different for, say, business-as-usual trajectories of emissions or even socially optimal trajectories of emissions that do not incorporate concerns about uncertainty. Thus, our decompositions are of potential interest for emissions trajectories other than those chosen as part of a solution to an uncertainty averse planner's problem.

9 A richer economic setting

While our main analysis has so far focused on a stylized model of the coupled climate-economy dynamics, our framework is also well-suited for exploring richer environments. Important modeling extensions include additional macroeconomic components that allow for adaptation, technological change, and multiple sectors. We have left off the table discussions of technological innovation that could support the transition from dirty to clean capital and the reallocating production from technologies that are vulnerable to climate change to ones that are more resilient. Modeling extensions that allow us to address a broader range of economic responses are important both for assessing the role of policy and for accommodating market responses. Rather than constructing an all purpose integrated assessment model, we describe a two-capital model setup that allows us to confront some of the gaps left with our illustrative model.

We take as starting point the two capital, AK specification of Eberly and Wang (2012) that includes adjustment costs and hence sluggish reallocation. The resulting technologies are stochastic subject to Brownian increment shocks and are used to output that is divided between investment and consumption. It is a two capital extension of the undamaged consumption/investment model that we have used so far. Although their model has stochastic growth, many parameter configurations imply long-term stationary behavior of the relative capital stocks. The ratio of the capital stock becomes a featured state variable for their model. We start with two capital stocks that evolve as:

$$dK_{j,t} = K_{j,t} \left[\mu_{j,k}(Z_t) \cdot dt + \left(\frac{I_{j,t}}{K_{j,t}} \right) dt - \frac{\kappa_j}{2} \left(\frac{I_{j,t}}{K_{j,t}} \right)^2 dt + \sigma_{j,k}(Z_t) \cdot dW_t^k \right]$$

and $K_{j,t}$ and $I_{j,t}$ are technology specific capital and investment for $i = 1, 2$. The output of each production is proportional:

$$I_{j,t} + C_{j,t} = \alpha_j K_{j,t}$$

For our first application, the planner has an instantaneous utility function that can be represented as:

$$\log \left[(C_{1,t})^{1-\eta} (\mathcal{E}_{1,t})^\eta + (C_{2,t})^{1-\eta} (\mathcal{E}_{2,t})^\eta \right] - (1-\eta) \log N_t$$

where the two sources of emissions contribute to damages differentially. Here, we have in mind coal and oil where coal use generates more emissions, and therefore leads to more climate damages than oil. In the absence of climate change considerations, both technologies are attractive sources of production. Taking account of climate change, a planner will shift production to the cleaner of the two technologies. This model opens the door to considering uncertainty and policy as it pertains to taxing or restraining coal production.

Next, we change the configuration to consider clean versus dirty technologies. To do so, we drop emissions from the second technology and replace it by an input available in fixed supply, τ . The resulting instantaneous utility function is of the form:

$$\log \left[(C_{1,t})^{1-\eta} (\mathcal{E}_{1,t})^\eta + (C_{2,t})^{1-\eta} \tau^\eta \right] - (1 - \eta) \log N_t$$

We suppose initially that there is a productivity advantage for the dirty technology, but that there is a third investment opportunity devoted to research and development (R&D) that can induce improvements in the production from the green sector. The outcome of accumulated R&D investment is the eventual stochastic arrival of a more productive green technology where the arrival is modeled as a jump process with intensity linked to the current stock of R&D. This setting is reminiscent of the framework explored by Acemoglu et al. (2016), though their focus is on the dynamics of innovation abstracting from capital reallocation and concerns about uncertainty. This second application opens the door to studying potential subsidies for R&D in the face of broadly conceived uncertainty.

As a third application, we suppose that one of the two production technologies is vulnerable to climate change while the other one is not. Consumption and investment from the two technologies are treated as perfect substitutes. We add an additional source of damages that might be triggered in the future but for only the first technology. Thus, the first technology is more vulnerable to climate change, as there is a productivity decline with an uncertain arrival time that becomes more likely as temperature increases. Given the sluggishness in reallocating capital, there can be non-trivial transitional consequences to this drop in productivity. This setting allows us to explore the role of policy for monitoring or limiting this vulnerability in the presence of damage uncertainties. See Fant et al. (2020) and Kling et al. (2021) for recent research quantifying vulnerability of productive activities to climate change and the potential need for adaptation. In a different vein, valuable quantitative research has been done building probabilistic models of climate tipping points and assessing their risk consequences. See, for instance, Lenton et al. (2008) and Cai et al. (2015). A model such as the one we described opens the door to the study of heterogeneous vulnerability to tipping point uncertainty conceived of more broadly than is typical in risk analyses.

While other studies have explored policy challenges introduced by related models, we will

study the broad consequences of uncertainty in such environments. In each case, we can include the analogous uncertainty concerns through model misspecification and ambiguity as before. By enriching the dynamics, however, we also open the door to new channels by which uncertainty comes into play and to alternative policy levers worthy of exploration.

10 Conclusion

In many dynamic settings, our understanding of the true underlying model relevant for economic decision-making is limited because existing evidence is weak along some important dimensions. As a result, the design and conduct of policy occurs in settings in which policy outcomes are uncertain. We offer the economics of climate change as an example, but there are many others. We turned to decision theory under uncertainty to serve as a guide for how we conduct uncertainty quantification as it contributes to the design of policy. Furthermore, we showed how different forms of uncertainty impact our quantification and provide a novel decomposition of the effects of uncertainty which we use to highlight the relative importance of sources of uncertainty for the determination of optimal policy by a social planner or policymaker.

Our analysis in this paper is made simpler here by posing the resource allocation problem as one faced by a single policy maker or social planner. To push closer to a realistic policy setting, multiple decision makers come into play, including alternative policy makers as well as private sector consumers and investors. Since these different agents confront uncertainty from different perspectives, their uncertainty concerns are expressed in different ways. Moreover, in more realistic policy settings, political constraints prevent first-best solutions. While we fully appreciate the need to extend our analysis of uncertainty to address these modeling challenges, we have little reason to doubt that the uncertainty considerations should remain as first-order concerns and not be shunted to the background as they often are in policy discussions.

References

- Acemoglu, Daron, Ufuk Akcigit, Douglas Hanley, and William Kerr. 2016. Transition to clean technology. *Journal of Political Economy* 124 (1):52–104.
- Anderson, Evan W, Lars Peter Hansen, and Thomas J Sargent. 2003. A quartet of semigroups for model specification, robustness, prices of risk, and model detection. *Journal of the European Economic Association* 1 (1):68–123.
- Arrhenius, Svante. 1896. On the influence of Carbonic Acid in the Air upon Temperatue of the Ground. *Philosophical Magazine and Journal of Science Series 5* 41:237–276.
- Bansal, Ravi and Amir Yaron. 2004. Risks for the Long Run: A Potential Resolution of Asset Pricing Puzzles. *Journal of Finance* 59 (4):1481–1509.
- Barnett, Michael, William A. Brock, and Lars Peter Hansen. 2020. Pricing Uncertainty Induced by Climate Change. *Review of Financial Studies* 33 (3):1024–1066.
- Cai, Yongyang, Kenneth L Judd, Timothy M Lenton, Thomas S Lontzek, and Daiju Narita. 2015. Environmental Tipping Points Significantly Affect the Cost-Benefit Assessment of Climate Policies. *Proceedings of the National Academy of Sciences* 112 (15):4606–4611.
- Cai, Yongyang, Kenneth L. Judd, and Thomas S. Lontzek. 2017. The Social Cost of Carbon with Climate Risk. Tech. rep., Hoover Institution, Stanford, CA.
- Cerreia-Vioglio, Simone, Lars Peter Hansen, Fabio Maccheroni, and Massimo Marinacci. 2021. Making Decisions under Model Misspecification.
- Chernoff, H. 1952. A Measure of the Asymptotic Efficiency for Tests of a Hypothesis Based on the Sum of Observations. *Annals of Mathematical Statistics* 23:493–507.
- Dietz, Simon and Frank Venmans. 2019. Cumulative carbon emissions and economic policy: In search of general principles. *Journal of Environmental Economics and Management* 96:108–129.
- Eberly, Janice C and Neng Wang. 2012. Reallocating and Pricing Illiquid Capital: Two Productive Trees. Tech. rep., SSRN Electronic Journal.
- Eby, M., K. Zickfeld, A. Montenegro, D. Archer, K. J. Meissner, and A. J. Weaver. 2009. Lifetime of anthropogenic climate change: Millennial time scales of potential CO₂ and surface temperature perturbations. *Journal of Climate* 22 (10):2501–2511.
- Epstein, Larry G. and Stanley E. Zin. 1989. Substitution, Risk Aversion and the Temporal Behavior of Consumption and Asset Returns: A Theoretical Framework. *Econometrica* 57 (4):937–969.
- Fant, Charles, Brent Boehlert, Kenneth Strzepek, Peter Larsen, Alisa White, Sahil Gulati, Yue Li, and Jeremy Martinich. 2020. Climate Change impacts and Costs to U.S. Electricity Transmission and Distribution Infrastructure. *Energy* 195.

- Geoffroy, O, D Saint-Martin, D J L Olivié, A Voldoire, G Bellon, and S Tytéca. 2013. Transient Climate Response in a Two-Layer Energy-Balance Model. Part {I}: Analytical Solution and Parameter Calibration Using CMIP5 AOGCM Experiments. *Journal of Climate* 26 (6):1841–1857.
- Ghil, Michael and Valerio Lucarini. 2020. The Physics of Climate Variability and Climate Change. *Reviews of Modern Physics* in press.
- Golosov, Mikhail, John Hassler, Per Krusell, and Aleh Tsyvinski. 2014. Optimal Taxes on Fossil Fuel in General Equilibrium. *Econometrica* 82 (1):41–88.
- Good, Irving J. 1952. Rational Decisions. *Journal of the Royal Statistical Society. Series B (Methodological)* 14 (1).
- Hansen, Lars Peter and Jianjun Miao. 2018. Aversion to Ambiguity and Model Misspecification in Dynamic Stochastic Environments. *Proceedings of the National Academy of Sciences* 115 (37):9163–9168.
- Hansen, Lars Peter and Thomas J. Sargent. 2001. Robust Control and Model Uncertainty. *The American Economic Review* 91 (2):60–66.
- . 2007. Recursive Robust Estimation and Control without Commitment. *Journal of Economic Theory* 136 (1):1–27.
- . 2020a. Macroeconomic Uncertainty Prices when Beliefs are Tenuous. *Journal of Econometrics* published online.
- . 2020b. Structured Ambiguity and Model Misspecification. *Journal of Economic Theory* published:105165.
- Hansen, Lars Peter, John C. Heaton, and Nan Li. 2008. Consumption Strikes Back? Measuring Long-Run Risk. *Journal of Political Economy* 116 (2):260–302.
- Hassler, John, Per Krusell, and Conny Olovsson. 2018. The Consequences of Uncertainty: Climate Sensitivity and Economic Sensitivity to the Climate. *Annual Review of Economics* 10:189–205.
- Hotelling, Harold. 1931. The Economics of Exhaustible Resources. *Journal of Political Economy* 39 (2):137–175.
- James, Matthew R. 1992. Asymptotic Analysis of Nonlinear Stochastic Risk-Sensitive Control and Differential Games. *Mathematics of Control, Signals and Systems* 5 (4):401–417.
- Joos, F., R. Roth, J. S. Fuglestedt, G. P. Peters, I. G. Enting, W. Von Bloh, V. Brovkin, E. J. Burke, M. Eby, N. R. Edwards, T. Friedrich, T. L. Frölicher, P. R. Halloran, P. B. Holden, C. Jones, T. Kleinen, F. T. Mackenzie, K. Matsumoto, M. Meinshausen, G. K. Plattner, A. Reisinger, J. Segschneider, G. Shaffer, M. Steinacher, K. Strassmann, K. Tanaka, A. Timmermann, and A. J. Weaver. 2013. Carbon Dioxide and Climate Impulse Response Functions for the Computation of Greenhouse Gas Metrics: A Multi-Model Analysis. *Atmospheric Chemistry and Physics* 13 (5):2793–2825.

- Klibanoff, P, M Marinacci, and S Mukerji. 2009. Recursive {Smooth} {Ambiguity} {Preferences}. *Journal of Economic Theory* 144:930–976.
- Kling, Gerhard, Ulrich Volz, Victor Murinde, and Sibel Ayas. 2021. The Impact of Climate Vulnerability on Firms’ Cost of Capital and Access to Finance. *World Development* 137.
- Kreps, David M. and Evan L. Porteus. 1978. Temporal Resolution of Uncertainty and Dynamic Choice. *Econometrica* 46 (1):185–200.
- Lenton, Timothy M, Hermann Held, Elmar Kriegler, Jim W Hall, Wolfgang Lucht, Stefan Rahmstorf, and Hans Joachim Schellnhuber. 2008. Tipping Elements in the Earth’s Climate System. *Proceedings of the National Academy of Sciences* 105 (6):1786–1793.
- Maccheroni, Fabio, Massimo Marinacci, and Aldo Rustichini. 2006. Dynamic Variational Preferences. *Journal of Economic Theory* 128 (1):4–44.
- MacDougall, Andrew H., Neil C. Swart, and Reto Knutti. 2017. The Uncertainty in the Transient Climate Response to Cumulative CO₂ Emissions Arising from the Uncertainty in Physical Climate Parameters. *Journal of Climate* 30 (2):813–827.
- Matthews, H Damon, Nathan P Gillett, Peter A Stott, and Kirsten Zickfeld. 2009. The proportionality of global warming to cumulative carbon emissions. *Nature* 459 (7248):829–832.
- McGlade, Christophe and Paul Ekins. 2015. The geographical distribution of fossil fuels unused when limiting global warming to 2 C. *Nature* 517 (7533):187–190.
- Morgan, M. Granger, Parth Vaishnav, Hadi Dowlatabadi, and Ines L. Azevedo. 2017. Rethinking the Social Cost of Carbon Dioxide. *Issues in Science and Technology* 33 (4).
- Nordhaus, William. 2018. Projections and uncertainties about climate change in an era of minimal climate policies. *American Economic Journal: Economic Policy* 10 (3):333–360.
- Olson, Roman, Ryan Sriver, Marlos Goes, Nathan M. Urban, H. Damon Matthews, Murali Haran, and Klaus Keller. 2012. A Climate Sensitivity Estimate using Bayesian Fusion of Instrumental Observations and an Earth System Model. *Journal of Geophysical Research Atmospheres* 117 (D04103):1–11.
- Palmer, Tim and Bjorn Stevens. 2019. The scientific challenge of understanding and estimating climate change. *Proceedings of the National Academy of Sciences* 116 (49):24390–24395.
- Pierrehumbert, Ramond T. 2014. Short-Lived Climate Pollution. *Annual Review of Earth and Planetary Science* 42:341–379.
- Pindyck, Robert S. 2013. Climate Change Policy: What Do the Models Tell Us? *Journal of Economic Literature* 51 (3):860–872.
- Ricke, Katharine L. and Ken Caldeira. 2014. Maximum Warming Occurs about One Decade After a Carbon Dioxide Emission. *Environmental Research Letters* 9 (12):1–8.

Seshadri, Ashwin K. 2017. Fast–slow climate dynamics and peak global warming. *Climate Dynamics* 48 (7-8):2235–2253.

Wagner, Gernot and Martin Weitzman. 2015. *Climate Shock*. Princeton University Press.

Weitzman, Martin L. 2012. GHG Targets as Insurance Against Catastrophic Climate Damages. *Journal of Public Economic Theory* 14 (2):221–244.

Appendix A Carbon and Temperature Model Sets

As mentioned previously, we use 16 models of temperature dynamics from Geoffroy et al. (2013) and nine models of carbon dynamics models from Joos et al. (2013). We briefly describe the model experiments used in these papers, list the models we include in our analysis, and provide details for the reader to find additional information about these models and model experiments.

Geoffroy et al. (2013) approximates the temperature dynamics of 16 different models using a two-layer energy-balance model (EBM) to study properties of atmosphere-ocean general circulation models (AOGCMs). Table 1 lists the model name for each of the 16 models used in their and our analysis and direct the reader to Geoffroy et al. (2013) and Seshadri (2017) for additional details about each of the models.

The Geoffroy et al. (2013) EBM model uses the following specification:

$$\begin{aligned} c_s \frac{dT^s}{dt} &= F - \gamma T^s - \epsilon \chi (T^s - T^o) \\ c_o \frac{dT^o}{dt} &= -\chi (T^o - T^s) \\ F &= 5.35 (\log CO_2 - \log \underline{CO_2}) \end{aligned}$$

where T^s is the surface temperature, T^o is the ocean temperature, CO_2 is atmospheric carbon dioxide, and $\underline{CO_2}$ is the preindustrial benchmark. The construction of F comes from the ‘‘Arrhenius’’ equation (Arrhenius (1896)). The EBM model is solved for explicit solutions, calibrated to fit the responses of 16 AOGCMs that participated in the CMIP5, and then validated by using the AOGCM responses to the linear forcing experiments of one percent of CO_2 per year. The parameters they estimate in this simplified representation differ depending on the model used in the calibration of the approximation, providing a measure of the heterogeneity and uncertainty present in models of temperature dynamics. We use this specification along with Geoffroy et al.’s estimates of the 16 temperature dynamics models in our simulations to capture the carbon-to-temperature component of climate model uncertainty.

Joos et al. (2013) use a carbon cycle-climate model intercomparison analysis to study the impulse response time-scales of Earth System models. From their analysis, we use the impulse response functions of nine models based on a 100GtC emission pulse added to a constant CO_2 concentration of 389 ppm.¹⁶ All of the models we use are Earth System Models of Intermediate Complexity, except for the reduced form model Bern-SAR. We list the model name for each of the models used in our analysis in Table 2 below. We direct the reader to Appendix A in Joos et al. (2013) for detailed descriptions of these and other models used in their intercomparison analysis.

¹⁶We acknowledge Fortunat Joos for graciously providing the data for these and other response experiments on his website: https://climatehomes.unibe.ch/~joos/IRF_intercomparison/results.html.

Temperature Dynamics Models
BCC-CSM1-1
BNU-ESM
CanESM2
CCSM
CNRM-CM5
CSIRO-Mk3.6.0
FGOALS-s2
GFDL-ESM2M
GISS-E2-R
HadGEM2-ES
INM-CM4
IPSL-CM5A-LR
MIROC
MPI-ESM-LR
MRI-CGCM3
NorESM1-M

Table 1: List of temperature dynamics models from Geoffroy et al. (2013) and Seshadri (2017) used in our analysis.

Carbon Dynamics Models
Bern3D-LPJ (reference)
Bern2.5D-LPJ
CLIMBER2-LPJ
DCESS
GENIE (ensemble median)
LOVECLIM
MESMO
UVic2.9
Bern-SAR

Table 2: List of carbon dynamics models from Joos et al. (2013) used in our analysis.

Appendix B Solving for the value function components

In Section 6, we discussed a climate economics HJB equation in the state variable y . This is part of a larger system that can be solved with two additional subsystems of equations. The three subsystem solutions, when combined, give a solution to the composite HJB equation of the planner.

B.1 Climate economics system parameters

Parameter	Value
ζ'	[2.23 0]
γ_1	.000177
γ_2	.0044
γ_3^1	.000
γ_3^2	.039
γ_3^3	.771
η	.032
δ	.01

Table 3: Climate economics system parameters

To understand better the implications of the ζ specification note that for a constant emissions path, the implied standard deviation associated with the coefficient of the Matthew's approximation is .446 at twenty five years, .315 for fifty years and .223 for one hundred years.

B.2 Consumption-capital dynamics

The undamaged version of consumption capital model, by design, has a straightforward solution. We use the “guess and verify” method to derive a solution for this subsystem, guessing a value function of $v_k \log k + \zeta(z)$. The HJB equation for this component is:

$$\begin{aligned}
 0 = & \max_i \min_h -\delta [v_k \log k + \zeta(z)] + (1 - \eta) [\log(\alpha - i) + \log k] + \frac{\xi_b}{2} |h|^2 \\
 & + v_k \left[\mu_k(z) + i - \frac{\kappa}{2} (i)^2 + \sigma_k(z)'h - \frac{|\sigma_k(z)|^2}{2} \right] \\
 & + \frac{\partial \zeta}{\partial z}(z) [\mu_z(z) + \sigma(z)'h] + \frac{1}{2} \text{trace} \left[\sigma(z)' \frac{\partial^2 \zeta}{\partial z \partial z'}(z) \sigma(z) \right]
 \end{aligned}$$

From this equation, we derive the constant scaling the capital component of the value function v_k and can see that it must be

$$v_k = \frac{1 - \eta}{\delta}.$$

Solving for the first-order conditions, we see that the first-order condition for h is

$$\xi_b h + \sigma_k v_k + \sigma_z \frac{\partial \zeta}{\partial z} = 0,$$

and the first-order conditions for the investment-capital ratio is

$$-(1 - \eta) \left(\frac{1}{\alpha - i} \right) + v_k (1 - \kappa i) = 0.$$

Notice that the equation for the optimal h is therefore

$$h = -\frac{1}{\xi_b} \left[\sigma_k v_k + \sigma_z \frac{\partial \zeta}{\partial z} \right]$$

and that the investment-capital ratio is constant. While there are two solutions for the first-order conditions for i , only one is positive. In our illustration we set $\alpha = .115$ and $\kappa = 6.667$.

The solution for h will be state dependent if we allow for σ_k or σ_z to depend on z or if there is nonlinearity in the drift specifications. Such dependence is common in the macro finance literature as a form of stochastic volatility. In the computations that follow, we will abstract from this dependence and impose linear dynamics for z . We impose that

$$\mu_k(z) = -.043 + .04(\iota_k \cdot z)$$

and

$$\sigma_k = .01 \begin{bmatrix} .87 & .38 \end{bmatrix} dW_t^k$$

where dW^k is a two dimensional subvector of the Brownian increment vector dW . The evolution for the process $\iota_k \cdot Z$ is given by a continuous-time autoregression:

$$d(\iota_k \cdot Z_t) = -.056 (\iota_k \cdot Z_t) dt + \begin{bmatrix} 0 & .055 \end{bmatrix} dW_t^k$$

In this case $\zeta(z) = \zeta_0 + \zeta_1 \iota_k \cdot z$ where ζ_1 satisfies

$$-\delta \zeta_1 + v_k (.04) + \zeta_1 (-.056) = 0.$$

The implied solution for h is constant and equal to:

$$h^* = -\frac{1}{\xi_b} \begin{bmatrix} .85 \\ 3.58 \end{bmatrix}$$

The implied consumption dynamics in this setting are consistent with the ones given in Hansen and Sargent (2020a):¹⁷

$$d \log C_t = .0194 + .04Z_t dt + .01 \begin{bmatrix} .87 & .38 \end{bmatrix} \cdot dW_t^k.$$

B.3 Contribution of $\iota_y \cdot z$

There is one remaining contribution to the planners HJB equation. Note that while $\log \iota_y \cdot z$ is included in the objective of the planner, this term has not been accounted for in our solution so far. Thus there is a third contribution, $\tilde{\zeta}$ to the value function that solves:

$$\begin{aligned} \min_h -\delta \tilde{\zeta}(z) - \eta \log(\iota_y \cdot z) + \left[\frac{\partial \tilde{\zeta}}{\partial z}(z) \right] \cdot [\mu_z(z) + \sigma_z(z)h] + \frac{\xi_b}{2} h' h \\ + \frac{1}{2} \text{trace} \left[\sigma_z(z)' \frac{\partial^2 \tilde{\zeta}}{\partial z \partial z'}(z) \sigma_z(z) \right] = 0. \end{aligned} \quad (9)$$

To support this value function separation we impose that $\iota_y \cdot Z$ and $\iota_k \cdot Z$ are independent processes with $\iota_y \cdot Z$ constructed as a function of the dW^y increments and $\iota_k \cdot Z$ constructed in terms of the dW^k increments. Moreover, we assume that

$$\zeta' \sigma_z(z)' \left[\frac{\partial \tilde{\zeta}}{\partial z}(z) \right] = 0 \quad (10)$$

where $\tilde{\zeta}$ is the solution to HJB equation $\left[\frac{\partial \tilde{\zeta}}{\partial z}(z) \right]$.

As a special case suppose that $\iota_y \cdot Z_t$ evolves as Feller square root process with mean one:

$$d(\iota_y \cdot Z_t) = -\chi(\iota_y \cdot Z_t - 1)dt + \sqrt{\iota_y \cdot Z_t} \tilde{\zeta} \cdot dW_t^y.$$

where $\tilde{\zeta} \cdot \zeta = 0$. Then the solution of interest to equation (9) can be expressed as a functional equation in the scalar argument $\iota_y \cdot z$.

As part of a “guess and verify” solution method we add the three value function components and the three components for the minimizing h together along with the proposed solutions for the investment capital ratio i and for scaled emissions \tilde{e} . In fact there may be good reasons to relax

¹⁷Hansen and Sargent (2020a) represent the dynamics in terms of a time unit of one quarter instead of one year, and they report a different but observationally equivalent orthogonalization of the Brownian increments.

assumption (10) and combine the climate economics HJB contribution and that coming from (9) into a single HJB equation to be solved instead of two lower-dimensional functional equations.